Review

Journal of the Brazilian Chemical Society

https://dx.doi.org/10.21577/0103-5053.20240109

J. Braz. Chem. Soc. **2024**, *35*, 10, e-20240109, 1-35

Advancements in the Synthesis and Biological Properties of Carboranes and High-Boron Related Compounds: A Comprehensive Exploration with Emphasis on BNCT Applications

Marcos Couto *,[a] ***and Hugo Cerecetto*** *,[a,b]

[a]*Grupo de Química Orgánica Medicinal, Instituto de Química Biológica, Facultad de Ciencias, Universidad de la República, Iguá 4225, 11400 Montevideo, Uruguay*

[b]*Área de Radiofarmacia, Centro de Investigaciones Nucleares, Facultad de Ciencias, Universidad de la República, Mataojo 2055, 11400 Montevideo, Uruguay*

Since Locher proposed the concept of boron neutron capture therapy (BNCT) in 1936, it has become a great challenge in the field of medicinal chemistry. The great dare has been to obtain boron-containing compounds that selectively accumulate in the organ to be irradiated. Polyhedral boron clusters (PBC) have been considered attractive moieties for the development of BNCT-agents due to their large contribution of boron *per* molecule. Various issues arose in the first efforts to develop PBC during the 1940-1950s that prevented their application in BNCT clinical trials, such as a lack of selectivity and low boron tumor-accumulation. Currently, the most studied PBC in BNCT are the icosahedral dicarba-*closo*-dodecaboranes ($C_2B_{10}H_{12}$) commonly referred to carboranes and, to a lesser extent, their mono-anionic derivatives resulting from the loss of a B-vertex, commonly known as *nido*-carborane, and their metal complexes, known as metallacarboranes. This review will cover the medicinal chemistry of PBC for BNCT.

Keywords: boron-containing molecules, carborane, metallacarborane, boron neutron capture therapy (BNCT)

1. Introduction: Boron Neutron Capture Therapy (BNCT)

Four years after the discovery of neutrons, by the Nobel laureate J. Chadwick from Cavendish Laboratory at Cambridge University, the physicist Gordon L. Locher proposed the therapeutic possibilities of these uncharged elementary particles.[1] In this report, Locher mentioned that some elements have strong absorption of neutrons due to their particular nuclear structures, which make them particularly susceptible to nuclear "transmutation", mentioning lithium, boron, yttrium, mercury, samarium, and gadolinium among others, laying out the bases for neutron capture therapy (NCT). In his words "In the field of medical research … the direct application of neutrons … have occurred to me …. the possibility of destroying or weakening cancerous cells, by the general or selective absorption of neutrons by these cells. In particular, there exist the possibilities of introducing small quantities of strong neutron absorbers into the regions where it is desired to liberate ionization energy (a simple illustration would be the injection of a soluble, non-toxic compound of boron, lithium, gadolinium, or gold into a superficial cancer, followed by bombardment with slow neutrons".[1] Only two years later the first radiobiological experiments with tumor-bearing animals, dosing with boric acid and slow neutron bombardment, were carried out.[2]

Nowadays, the NCT is conceived as a binary radiotherapeutic tool for cancer treatment. The technique relies on the nuclear fission reaction triggered by low-energy thermal neutrons that hit to particular stable nuclides previously accumulated in cancerous cells. Research has mainly focused on ^{10}B stable nuclide as the neutron capture agent being ^{157}Gd a currently studied alternative nuclide for NCT.[3]

^{10}B, the non-radioactive nuclide constituent of natural

*e-mail: mcouto@fcien.edu.uy; hcerecetto@cin.edu.uy

Editor handled this article: Carlos Maurício R. de Sant'Anna (Guest)

With all our love for the scientist and friend, a reference in Ibero-American medicinal chemistry, Dr Eliezer Jesús de Lacerda Barreiro

elemental boron in approximately 20%, irradiated either with low-energy thermal (0.025 eV) or, for clinical studies, epithermal (0.5 eV to 40 keV) neutrons beam results in $^{10}B(n,\alpha)^{7}Li$ nuclear reactions, yielding excited boron-11 ($^{11}B^*$) that after instantaneous nuclear fission generates α-particles ($^{4}He^{2+}$, of ca. 1.47 MeV) and recoils $^{7}Li^{3+}$ (ca. 0.84 MeV) (Figure 1). These particles possess high linear energy transfer (LET), in the order of ca. 175 keV μm^{-1}, and the excited recoiling $^{7}Li^{3+}$ generally emit a low LET γ-ray during deexcitation. The generated charged-particles are characterized by high energy and short travel distances, < 5 μm for $^{7}Li^{3+}$ and < 10 μm for $^{4}He^{2+}$. Due to these short tracks length radiation damage is confined to those cells loaded with ^{10}B. The α-particles produce dense ionization tracks along biomacromolecules, such as deoxyribonucleic acid (DNA), producing, in comparison to low-LET radiation (X-rays, γ-radiation, electrons, positrons and muons), more complex damage characterized by co-localization of different forms of DNA damage-base excision, single strand-breaks, and, the most damaging, double-strand breaks. Furthermore, the effectiveness of BNCT lies in part in the fact that the value of the neutron capture cross-section on ^{10}B (which is proportional to the probability of a collision between the neutron and the boron nuclei), equal to σc = 3835 barn,[4] is much higher than the cross-sections of any interaction with abundant endogenous nuclides ^{12}C, ^{1}H or ^{14}N, being on the order of 4-20 barn. Consequently, BNCT could be a minimally invasive therapy if the ^{10}B accumulation were selective.[5]

1.1. BNCT in the context of medicinal chemistry

Cancer rips across society, affecting people of all ages, genders, and social classes causing suffering on a worldwide scale. One of the biggest challenges facing medicinal chemists, oncologists and the scientific community as a whole is to improve the therapeutic ratio of treatment by increasing cancer cell death while limiting the probability of normal tissue complications. In this sense, BNCT has been suggested to treat cutaneous melanomas, salivary gland carcinomas, head and neck tumors, multifocal hepatocellular carcinoma, recurrent lung cancer, squamous cell carcinomas, sarcomas, recurrent malignant meningioma, extra-mammary Paget's disease, and glioblastoma multiforme with a large number of clinical trials underway around the world.[6-11] For example, in 2020, BNCT was approved in Japan as a clinical therapy, covered by the National Health Insurance, for patients with recurrent or locally advanced head and neck cancers.[12] These advances are the result of the progress that Japan has made in developing appropriate technologies. The development of accelerator-based neutron sources with effective beam intensity for BNCT allows the installation of BNCT facilities *in situ*, overcoming one of the major obstacles for the bench-to-bedside transition of the BNCT, the access to a nuclear reactor in the hospital where patients would undergo the treatment.

The other major problem that must be resolved for an adequate application of BNCT is related to medicinal chemistry field, i.e., the selective delivery of therapeutic dose of boron to tumoral cells. In this sense, boron containing agents should meet the following requirements:[11,13] (*i*) near to 10^{9} ^{10}B-atoms should be delivered *per* cancer cell, that means approximately 20-40 μg of ^{10}B *per* weight (in g) of tumor; (*ii*) boron concentration ratios should be: tumor:blood > 3.5 and tumor:normal tissue ≥ 3; (*iii*) the ^{10}B should be retained into the tumoral tissue at least for the duration of neutron-irradiation, which could take up near to an hour; (*iv*) boron particular intracellular localization, i.e., nuclear location, is preferred to maximize DNA damage upon irradiation; (*v*) low toxicity and fast clearance from healthy tissues and blood after the treatment; (*vi*) other drug-like properties have to be: absence of side-effects, chemical and metabolic stability and water solubility. Therefore, the way to concentrate ^{10}B in sufficient amounts and selectively, by entities with suitable drug-like properties, in tumoral tissues is currently the main BNCT-medicinal chemistry goal.

1.2. Boron-containing compounds in BNCT

Boron has a wide range of applications in the field of chemistry, energy, materials and the biomedical sciences.[14] The use of organoboron derivatives as

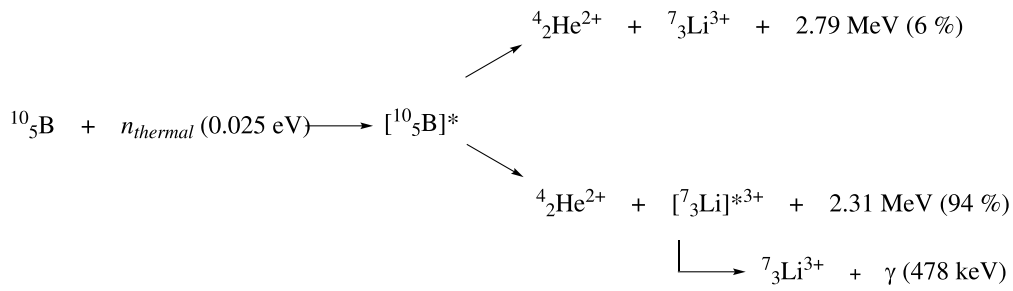

Figure 1. Nuclear fission reactions that occur upon capture of a slow (thermal) neutron by a ^{10}B nuclide.

potential agents for BNCT has a long history due to the few successful results with simple boron salts. In this sense,[15-17] borax (disodium tetraborate decahydrate, $Na_2B_4O_7{\cdot}10H_2O$), used in the first clinical trial in 1951, sodium pentaborate (NaB_5O_8) in combination with D-glucose and disodium decahydrodecaborate ($Na_2B_{10}H_{10}$) studied in patients undergoing BNCT (Figure 2), demonstrated have side effects, such as toxicity *per se*, radio-dermatoses of the scalp and deep ulcerations, and brain necrosis. Due to these disappointing events, the USA halted the progress of research on BNCT in 1961.[15-17]

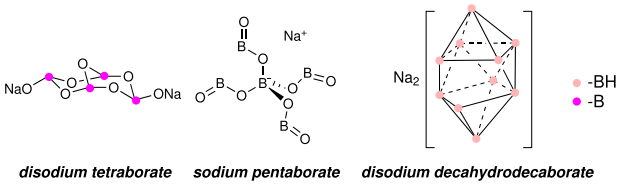

Figure 2. First boron-based drugs for BNCT.

Currently, one of the boron-delivery organo-derivative used in BNCT-treatment and -clinical trials is 4-borono-L-phenylalanine (BPA, or Borofalan[^{10}B] as generic name, or BPA D-sorbitol complex, launched in Japan in 2020) (Figure 3).[18] This is a boronic acid derived from L-phenylalanine that was designed in order to be recognized and uptaken by the tumoral tissue-overexpressed L-type amino acid receptors, i.e., LAT1. It is synthetically obtained as pure enantiomer in excellent yield and under mild conditions[19-22] and in clinical studies it was able to incorporate a maximum near to 37 μg of boron *per* gram of tumor when it was administered via intravenous infusion, during 2-3 h, at 500 mg of BPA *per* kg of patient body weight.[23] Some disadvantages regarding to BPA drug-like properties, such as solubility, metabolic stability, reaction with endogenous carbohydrates, have promoted its use as adduct with sugars, especially with D-fructose or D-sorbitol (Figure 3), which improves these properties. Another problem with BPA is that its short retention time in tumors decreasing during neutrons irradiation and compromising therapeutic effectiveness. This phenomenon seems to be the result of an efflux mechanism due to the exchange of amino acids, for example via LAT1, from intra- to extra-cellular location, i.e., the BPA cytosolic-entry may be associated with the extracellular-exit of glutamine and *vice versa*, antiport mechanism. To avoid this phenomenon different approaches have been described: (*i*) pre-administration of LAT1 substrates to enhance BPA tumor accumulation;[24] (*ii*) structural modifications, for example generation of adduct with poly(vinyl alcohol) (Figure 3), in order to enhance cellular uptake by slow-release from endo/lysosome and decrease the untoward efflux.[25,26]

Recently, the pharmacophores boronic acid, boronate ester and borate have been used to design and prepare new potential BNCT agents, from large molecules, such as antibodies, to polymers (BPA_2) and small ones (boron-based small molecule, BbSM_1-3) including the generation of hybrid compounds, chemical entities with two or more structural domains having different biological funcitons,[27] (BbSM_4, a boronate ester containing temozolomide) and theranostic agents (BPA_1, BbSM_5 and BPA_3) (Figure 3).[18,27-31]

The other agent that, since 1968, has been studied in BNCT clinical trials is disodium mercaptoundecahydro-*closo*-dodecaborate ($Na_2B_{12}H_{11}SH$, named as BSH; Figure 4).[32] It is a small polyhedral boron cluster that contains 12 times more B *per* molecule than BPA yielding, in a BNCT process, a higher number of events after neutron capture. Therapeutically it does not cross the intact blood-brain barrier penetrating into the brain passively when the barrier is disrupted, in many glioblastomas the pathology in which BSH is usually studied, reaching low tumor:blood and tumor:brain ratios, 0.9-2.5 and 3, respectively.[33]

The maximum value of boron concentration in tumors obtained in clinical studies is lower than the value for BPA, i.e., 19.9 μg of boron *per* gram of tumor when it was administered at a dose of 100 mg of BSH *per* kg of patient body weight infused and at a dose rate of 1 mg kg^{-1} min^{-1}.[34] BSH has high chemical and catabolic stability in the boron-cluster but it undergoes spontaneous dimerization in culture milieu to the corresponding disulfide, BSSB, and the strong cellular boron-retention is the result of the slower washout the boromercapto-dimeric form.[35] Some disadvantages regarding to BSH are: (*i*) lack of receptor-mediated selective transportation to cancer cells; (*ii*) poor pharmacokinetics and bioavailability; (*iii*) not economically viable preparation.

Medicinal chemistry on BSH, structural modifications, has also been done seeking better biological behavior (Figure 4).[36-38] Some of them showed excellent tumoral incorporation of boron, i.e., 69 μg of boron *per* gram of tumor when copolymer BSH_1 (Figure 4) was administered via the tail vein at a dose of 50 mg, on a BSH basis, *per* kg of mouse body weight; or a maximum near to 21 μg of boron *per* gram of tumor when BSH_2 (Figure 4) was administered by long term convection-enhanced delivery (CED) for 24 h at a dose of 1.2 mg of ^{10}B *per* kg of rat body weight; or 1.2 times more boron tumor-accumulation than BSH when BSH_3 (Figure 4) was administered in the same conditions that its parent compound.

Because of their high boron content *per* molecule, polyhedral boron clusters (PBC) have been regarded as

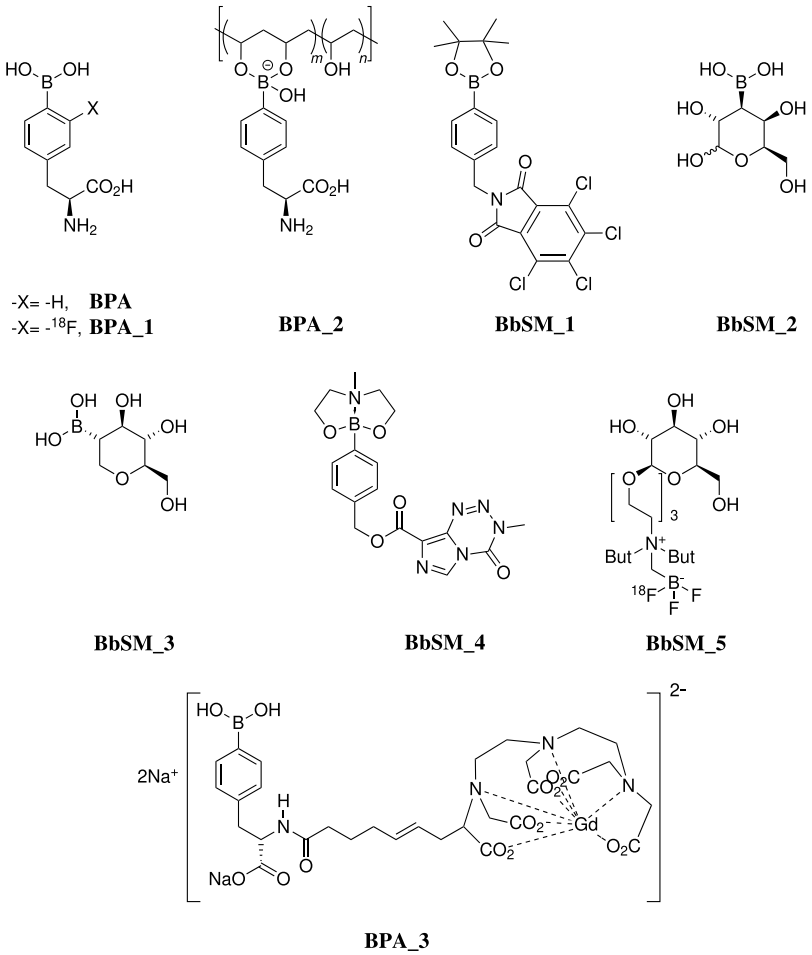

Figure 3. Recently developed BPA, boronic acid, boronate ester and borate derivatives under investigation as potential agents for BNCT and/or theranostic applications.

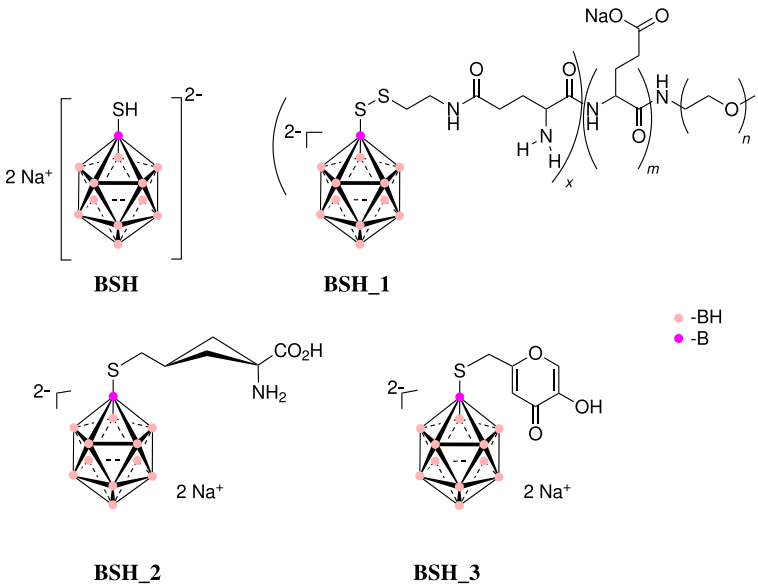

Figure 4. BSH and undecahydro-*closo*-dodecaborate derivatives recently developed and studied as potential BNCT agents.

desirable moiety for the creation of BNCT-agents. Since the initial description of BSH, currently the most studied PBC in BNCT are derivatives from: (*i*) the icosahedral dicarba-*closo*-dodecaborane ($C_2B_{10}H_{12}$), also known as carboranes;

(*ii*) their mono-anion produced from the loss of a B-vertex, called *nido*-carborane; (*iii*) and their metal complexes, called metallacarboranes, that are generated after removal of the bridge hydrogen from the *nido*-carborane. The following sections will provide a detailed description of these chemical systems.

2. Overview of Polyhedral Boron Compounds

The general structure of PBC, mainly icosahedral *closo*-borane and heteroborane clusters, like the inorganic icosahedral *closo*-dodecaborate ($[B_{12}H_{12}]^{2-}$, contained in BSH), the dicarba-*closo*-dodecaborane (*closo* $C_2B_{10}H_{12}$), known as carboranes, the mono-anionic derivatives resulting from the loss of a B-vertex known as *nido*-carborane ($[C_2B_9H_{12}]^-$), and the sandwich metallabis(dicarbollides) $[M(C_2B_9H_{11})_2]^-$ (M = Co^{3+}, Fe^{3+}) are discussed in the next sections. The term *closo* is used when the polyhedral is complete but *nido*-, *arachno*- and *hypho*- are used for one, two- or three-missing vertexes. On the other hand, the substituted or unsymmetrically-substituted metallabis(dicarbollides) exist in five distinct conformations: *cisoid*-1, *cisoid*-2, transoid, gauche-1 and gauche-2.[39]

2.1. Structure and bonding of boranes, carboranes and their derivatives

Boron, which is denoted by the symbol B, has unique qualities due to its positioning on the periodic table. As boron is carbon's leftward neighbor and a member of the 13th group and 2nd period, it has three valence electrons overall instead of one. Unlike its group's metals, it is a metalloid and can form covalent bonds similar to carbon and silicon. Its trivalent electronic configuration and the presence of an empty p orbital allow it to alternate between the neutral sp^2 and the anionic sp^3 hybridization states (Figure 5). Additionally, boron can form three-center two-electron (3c2e) boron-hydrogen-boron bonds, which enable a wide range of boron clusters to be made (Figure 5).[40]

Two stable nuclides are found in nature, ^{11}B (80.1%) and ^{10}B (19.9%), however, it does not occur in an elemental form, but rather forming borates such as borax ($Na_2B_4O_7.10H_2O$) and colemanite ($Ca_2B_6O_{11}.5H_2O$). The first documented chemical research related to boron dates from 1702, when W. Homberg synthesized boric acid starting from borax and iron(II) sulfate. In 1808, the French chemists Gay-Lussac and L. J. Thenard, and independently, the English Sir Humphry Davy, obtained elemental boron, although none of them recognized the substance as a new element, that would later be acknowledged by Jöns Jacob Berzelius in 1824. It is only in the year 1912, when based on the investigation carried out by the German chemist Alfred Stock, the first hydrogen and boron based compounds, boranes, were synthesized.[41,42]

2.1.1. Boranes

Boranes are diamagnetic, colorless, white or yellow molecular compounds, which are structured as polyhedral clusters of triangular faces with vertices formed exclusively by B–H units. They have the generic molecular formula $[B_nH_m]X^-$ and do not exist in nature. The preparation of these from minerals such as borax can be done by a wide variety of routes. Figure 6 shows some routes to obtain some boranes.

Lipscomb and co-workers[43,44] proposed for larger boranes that, in addition to the 2c-2e B–H and B–B linkage, open and closed 3c-2e bonds are involved between three B–B–B atoms where the atoms are arranged at the vertices of a triangle, generating a bonding molecular orbital (MO) in the center of it (Figure 7).

Lipscomb[43,44] allocated to four types of localized electron pair bonds using the styx rule, which includes as parameters the number of 2c-2e (x: B–H / y: B–B) and 3c-2e (s: B–H–B / t: B–B–B) bonds necessary to describe the stereochemistry of a borane. However, an especially useful, simple, and styx-rule-related tool for elucidating the structure of boranes and heteroboranes (where one or more boron vertex atoms in the cluster are replaced by C, N, O, Si, P, As, S, Se, Sb and/or Te) is the one developed in 1971 by Wade and Mingos,[53-56] Polyhedral Skeletal Electron

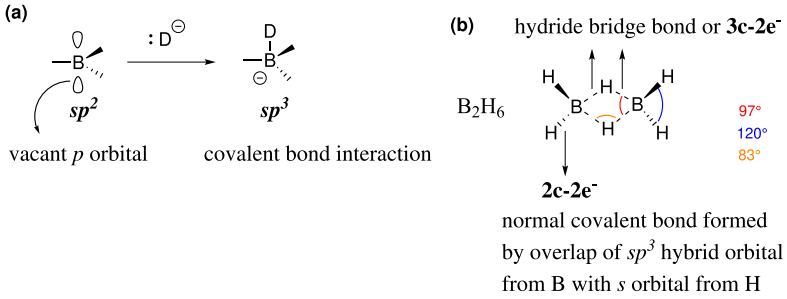

Figure 5. (a) sp^2-sp^3 hybridization states. (b) Non-classical bonding in B_2H_6, showing the three-center two-electron bonding characteristic of boron compounds.

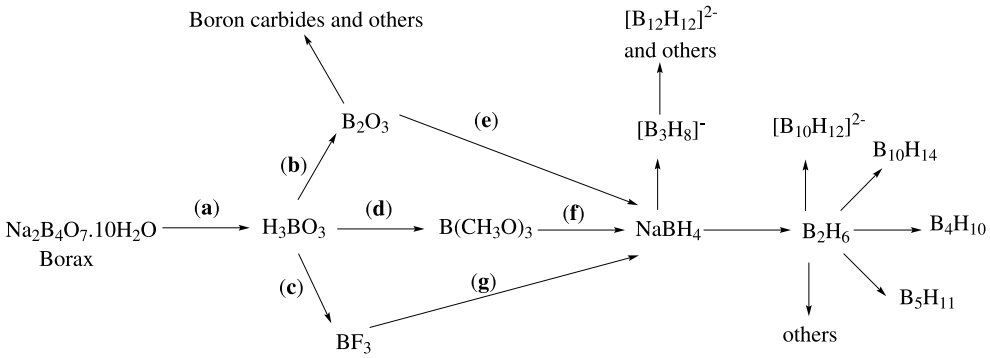

Figure 6. Simplified scheme for the preparation of some boranes from borax. (a) Synthesis of boric acid by treating borax with acid. H_3BO_3 can be transformed into boron oxide (B_2O_3) by calcination (b), boron trifluoride (BF_3) by treating with hydrogen fluoride (c), or trimethoxyborane $B(CH_3O)_3$ by esterifying H_3BO_3 with methanol. By these routes or others, sodium borohydride $NaBH_4$ can be obtained, by reducing with sodium hydride or by treatment with hydrogen and sodium (e, f, g), from which diborane B_2H_6 is synthesized by treating it with a Lewis acid. Higher boranes (polyhedral boranes or clusters) can be prepared from $NaBH_4$ and/or B_2H_6, such as tetraborane B_4H_{14},[45,46] pentaborane B_5H_{11},[45] triborane $[B_3H_8]^-$,[47] *closo*-decaborate $[B_{10}H_{10}]^{2-}$,[47,48] *nido*-decaborane ($B_{10}H_{14}$),[49] *closo*-dodecaborate $[B_{12}H_{12}]^{2-}$,[50-52] among others.

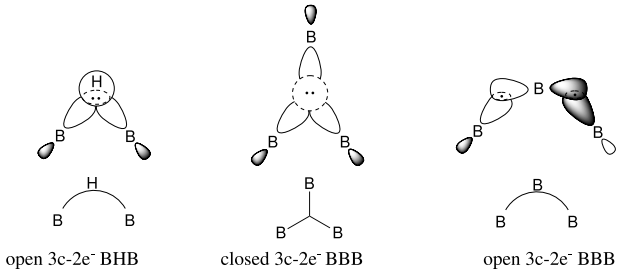

Figure 7. Bonds 3c-2e proposed by Lipscomb and co-workers.[43,44]

Pair Theory (PESEPT) colloquially known as "Wade's Rules" which are to this day important for the molecular compression of boron clusters.

Each boron-skeletal atom contained in polyhedral boranes constitutes a unit of boron possessing four atomic orbitals (AOs). Each boron-nucleus contributes to the cluster skeleton with three AOs, while the remaining AO is situated *exo*-cluster (B–H 2c-2e). Therefore, a cluster with n vertices contributes to its skeletal with 3n AOs to form MO. Taking *closo*-dodecaborate $[B_{12}H_{12}]^{2-}$ as an example (Figure 8a), theoretically predicted by Longuet-Higgins and Roberts in 1955,[57] the molecule would have 48 MOs (4 AOs for each vertex). Of the 48 MOs, the calculations predicted that 36 MOs (3n) are found distributed within or on the faces of the cluster (forming the skeleton), and the 12 MOs are oriented outside the cluster (*exo*-cluster), so they do not interfere directly in the structure of the skeleton. The 12 *exo*-cluster MOs would have one sp and $1e^-$ symmetry each, forming the B–H covalent bond. According to their calculations, of the 36 MOs of the skeleton, there are 13 bonding and 23 antibonding. Therefore, for the structure to be stable and *closo*-type, the 13 binding MOs (n + 1) of the skeleton would have to be filled with $26e^-$ (2n + 2). The 12 boron nuclei have a total of $12 \times 3e^- = 36e^-$ (of which $12e^-$ are already used in the *exo*-cluster links) and contribute $24e^-$ to the cluster skeleton (each vertex of the B–H cluster contributes $2e^-$ to the skeleton). A conclusion of this work[57] was that a borane of formula $B_{12}H_{12}$ would be stable only as a dianion $[B_{12}H_{12}]^{2-}$. This prediction was verified experimentally by Hawthorne and Pitochelli in 1960,[58] one year after they had prepared salts of the borane anion $[B_{10}H_{10}]^{2-}$. Thus, in the electronic structure of the boron clusters, it is considered that each boron vertex presents sp hybridization, where the s orbital and the p_z orbital combine to generate two sp_z hybrid AOs (one sp_z directed to the center of the cluster and the other towards outside) and there are two non-hybridized AOs, p_x and p_y, perpendicular to the sp_z and therefore tangential to the surface of the cluster (Figure 8b).

If a BH vertex (containing its two skeletal electrons) is removed from a *closo*-cluster (closed and triangular faces), a structure with an open face (*nido*) is formed, which to be stable requires compensating the same number of electrons that it had originally the *closo*. Therefore, although there

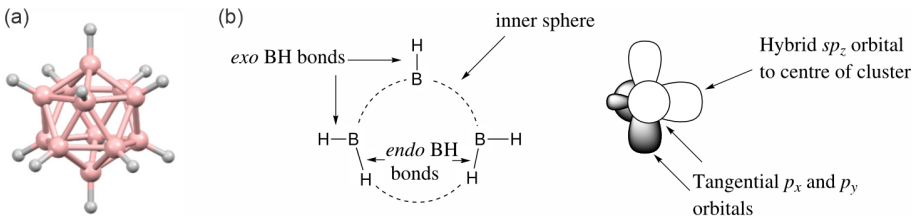

Figure 8. (a) 3D-structure of the $[B_{12}H_{12}]^{2-}$, B in pink and H in white; (b) structure of the boron clusters in terms of AOs (adapted from reference 59).

is one less vertex in the *nido* species, it can be said that it will be a cluster of n vertices and (2n + 4) electrons. If this operation is repeated by eliminating another BH vertex, a structure called *arachno* is formed, which will have a new value of n vertices but with (2n + 6) electrons contributed to the skeleton. Figure 9 shows the transformation of boron clusters published by Rudolph[60] based on Wade's Rules.

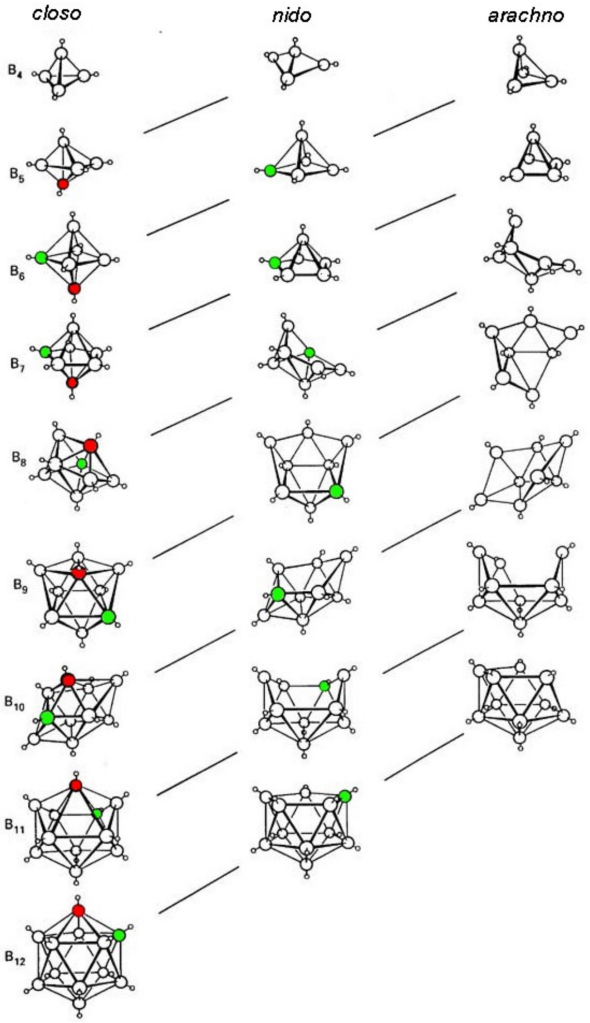

Figure 9. The deltahedral pattern in boranes and heteroboranes of the *closo* ($[B_nH_n]^{2-}$ or B_nH_{n+2}), *nido* (B_nH_{n+4}) and *arachno* (B_nH_{n+6}) type.

2.1.2. Carboranes

The substitution of one of the vertices in the boron clusters by a hetero-element gives rise to the family of heteroboranes, amongst which the carboranes, also known as carbaboranes, are the most studied ones, having at least one boron atom replaced by a carbon atom. The empiric formula of these compounds is: $[C_nB_mH_{n+m+p}]^{x-} = [(CH)_n(BH)_mH_p]^{x-}$, where n represents the number of C atoms within the vertices of the cluster, m is the number of B atoms within the cluster, p the number of bridging H (bridge H) and x the charge of de molecule. Of the four electrons that the carbon of a $C_{cluster}H$ vertex has, three electrons are contributed to the skeleton of the cluster, while the remaining one is located *exo*-cluster to form the hydrogen bond. Since $C_{cluster}H$ is isoelectronic with the $[B–H]^-$ group, if a $[B–H]^-$ vertex is formally replaced by a $C_{cluster}H$ in $[B_{12}H_{12}]^{2-}$, the monoanionic compound $[CB_{11}H_{12}]^-$ is obtained. When two vertices are replaced in $[B_{12}H_{12}]^{2-}$ by two $C_{cluster}H$ groups, dicarba-*closo*-dodecaborane is obtained, commonly known as carborane ($C_2B_{10}H_{12}$). The carborane comprises ten boron atoms and two carbon atoms, being each atom hexacoordinated. In total, 26 skeleton electrons are delocalized over the entire structure of the cluster, exhibiting σ aromaticity.[39,61,62] Three isomeric forms are known: *ortho*-, *meta*- and *para*-, which are differentiated by the relative position of the carbons in the cluster (Figure 10). At ca. 470 °C and in an inert atmosphere, *ortho*-carborane rearranges smoothly to 1,7-or *meta*-carborane (the two carbon atoms are separated by a boron atom) with near quantitative yields. *meta*-Carborane isomerizes further at ca. 620 °C to give 1,12-or *para*-carborane (the two carbon atoms are separated by two boron atom) although the yield is much smaller due to some cage degradation. The thermal stability of the isomers increases in the order *ortho* < *meta* < *para*.[63]

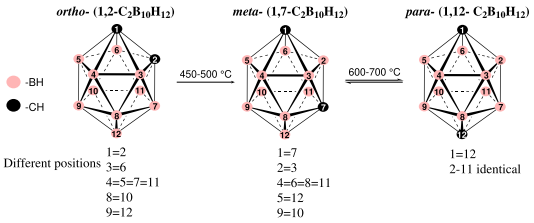

Figure 10. Graphical representation and thermal isomerization of the *closo*-carborane isomers ($C_2B_{10}H_{12}$) under inert conditions, with International Union of Pure and Applied Chemistry (IUPAC) numbering vertex. The solid and dashed lines are not to be regarded as classical two-center, two-electron single bonds.

2.2. Methods towards synthesizing polyhedral boron clusters (carborane, *nido*carborane and metallacarborane)

2.2.1. Synthesis of *ortho*-carboranes

One of the most common method to synthesize mono- and di-C-substituted *ortho*-carborane derivatives is the reaction of decaborane $B_{10}H_{14}$ with acetylenes in the presence of Lewis-base (CH_3CN, Et_2S, Et_3N, etc., Figure 11), though it is also commercially available nowadays.

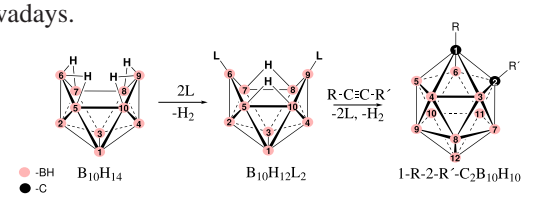

Figure 11. Synthetic scheme for *ortho*-$C_2B_{10}H_{12}$, starting with decaborane.

Terminal and internal alkynes typically have low yields (below 75%) and long reaction times; to address this issue, certain authors[64] have proposed alternative approaches for dehydrogenative alkyne-insertion of decaborane into biphasic ionic-liquid/toluene mixtures, which enable rapid reaction kinetics without the necessity of a Lewis base catalyst, or the use of some metallic catalyst. However, the chemistry community has not yet fully utilized this strategy, despite its potential.

From these simple systems other *o*-carboranes could be obtained taking advantage of the reactivity of the different clusters' vertices. Carborane clusters are known to exhibit different electronic effects on the substituents attached to different vertices. Due to a non-uniform electron distribution and the different electronegativities of boron (2.04), carbon (2.55), and hydrogen (2.20), according to Paulling scale, the cluster unit usually displays a strong electron-withdrawing character (which decreases in the order *ortho*- to *meta*- to *para*-carborane) with regard to substituents on the carbon atoms, whereas substituents at boron atoms antipodal to carbon atom experience an electron-donating effect. The B–H bonds suffers, via different potential reaction mechanisms,[65] electrophilic substitution reactions in the order of the charge distributions on *ortho*-carborane: B(9,12) > B(8,10) > B(4,5,7,11) >> B(3,6) (Figure 12). Consequently, Lewis acid mediated halogenation or alkylation are preferentially seen at cage B(9,12)–H bonds,[39,66] while the least electron-deficient B(3,6)–H bonds do not react to electrophilic substitution. These reactions allowed generating new carborane-derivatives.

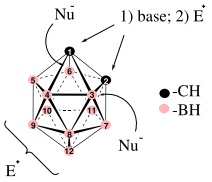

Figure 12. Reactivity of CH and BH vertices against strong bases, nucleophiles (Nu^-) and electrophiles (E^+).

2.2.2. Synthesis of *nido*carboranes: boron-cluster deboronation reaction

The carborane (mainly the *ortho* isomer) has long been known to be susceptible to strong Lewis bases such as alkoxides,[67] amines[68] and fluorides[69-72] to form salts of the anion *nido*-7,8-$C_2B_9H_{12}$. Deboronation, commonly referred as "decapitation" is initialized by attack of a base molecule on the most electropositive boron atom (B3/B6 in the *ortho*-carborane).[73,74] The next step involves cleaving a boron atom from the cluster with a second base molecule combined with a proton from the base (e.g., primary or secondary amines) or from the solvent (e.g., alcohols, water).[75] The process of removing a boron atom from the carborane cluster framework (Figure 13), leaves the cluster with an open pentagonal face, C_2B_3, is described as deboronation and does not necessarily result in the complete separation of a boron atom from a carborane molecule (see intermediate in Figure 13).

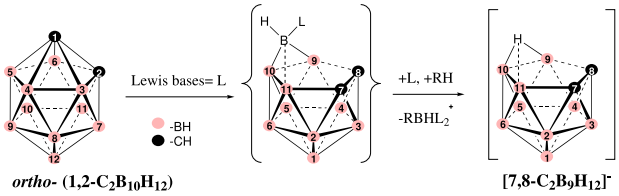

Figure 13. Partial degradation reactions of *ortho*-carborane with base L to obtain *nido*-carborane [7,8-$C_2B_9H_{12}$]$^-$ by going through the non-deboronated intermediate.

2.2.3. Synthesis of metallacarboranes: complexation reactions

The hydrogen atom located on the open face C_2B_3 of the *nido* cluster [7,8-$C_2B_9H_{12}$]$^-$, called pontal hydrogen or endo-hydrogen, is acidic and can be eliminated in a strongly basic aqueous medium or in anhydrous medium with *n*-BuLi, NaH or *t*-BuOK (Figure 14). Once this pontal hydrogen has been eliminated, a dianionic *nido* cluster is obtained, with the empirical formula $[C_2B_9H_{11}]^{2-}$, which is called dicarbollide. Due to the isolobal analogy between the cyclopentadienyl(−1) ligand and dicarbollide di-anion $[C_2B_9H_{11}]^{2-}$ (which behaves as a η5 ligand) it was thought that it could be suitable for complexing with transition metals (Figure 14). This is how in 1965 Hawthorne *et al.*[76] obtained the first sandwich type metallacarborane where two dicarbollide ligands complexed an iron atom, obtaining [3,3'-Fe(1,2-$C_2B_9H_{11}$)$_2$]$^-$, where iron has an oxidation state +3, commonly known as FESAN = FE sandwich.[76] Another of the most widely explored mixed-sandwich-type transition metal complexes in medicine includes the metallacarborane COSAN, which has Co^{III} as its metallic center (Figure 14).

In 2019, Viñas and co-workers[77] reported a new synthesis methodology in the absence of solvent that allows, from *ortho*- and *meta*-carborane, to generate the Co-bisdicarbollide complex. The protocol involve an easy, one-pot route to synthesize the pristine $[Co(C_2B_9H_{11})_2]^-$ and their $C_{cluster}$-substituted derivatives in a high yield in a rapid and efficient reaction. The solvent-free reaction between *nido* $[HNMe_3][7,8\text{-}C_2B_9H_{12}]$ and $CoCl_2.0.6H_2O$ were carried out by heating the two solid reagents at 350 ºC (also at 250 ºC) into a Pyrex tube.

For metallacarboranes, the polarity between the carbon and boron vertices due to the higher electronegativity of carbon (2.55 *vs.* 2.04, respectively) leads electrons to concentrate near the carbon atoms. This influences the

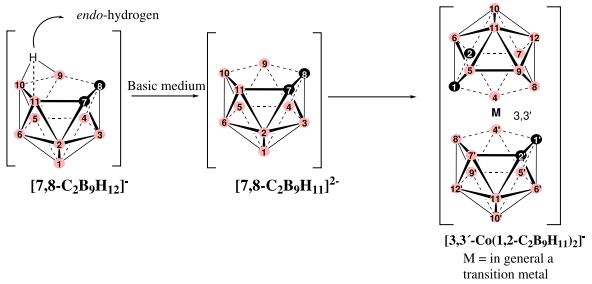

Figure 14. General scheme for the synthesis of metalladicarbollide.

different reactivity found for C and B, which allows the rich chemistry found in these clusters (Figure 15). Direct substitutions in the boron atoms[78,79] have been much more studied than substitutions in the carbon atoms. A way to derivatize the complex [3,3'-Co(1,2-$C_2B_9H_{11})_2]^-$ in the B–H vertices it is the electrophilically induced nucleophilic substitution (EINS), which takes advantage of the fact that in the B(8) or B(8') vertex there is the most hydride or electron-rich hydrogen and this reacts with strong acids, producing its elimination and subsequently the vacant position is occupied *in situ* by the nucleophile. Through this reaction, a wide range of metallacarboranes have been prepared, mainly incorporating the oxonium cycle linked to the B8/8' vertex, generating zwitterionic species of COSAN or FESAN. The metalla-based zwitterionic species has been proven to be susceptible to nucleophilic attack on the $-CH_2$ group, bonded to the positively charged oxygen atom (Figure 16).[80-87]

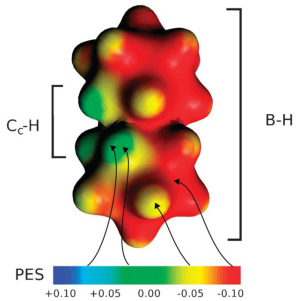

Figure 15. Electrostatic potential on the van der Waals surface of the *cisoid*-rotamer of [3,3'-Co-(1,2-$C_2B_9H_{11})_2]^-$ (reproduced from reference 88 with copyright permission 2010 from John Wiley and Sons).

2.3. Synthetic methods for icosahedral neutral dicarboranes functionalization: at the $C_{cluster}$–H vertices and at the B–H vertices

2.3.1. Carbon substitutions

Because the protons of the carbon atoms are mildly acidic, they can be attacked at low temperatures by organometallic bases like *n*-butyllithium or methyllithium to form the C-mono- or di-lithiocarborane. These bases then react with RX electrophiles to produce the corresponding substitution in the $C_{cluster}$ (Figure 17). The acidity of protons decreases in the order of *ortho*-, *meta*-, and *para*-carborane (pK_a values ca. 23, 28, and 30, respectively),[89] and is significantly influenced by substituents at the carbon or boron vertices of the clusters. For example, halogen atoms substituted clusters have drastically increased acidity of the C–H units.[64,90]

Mono- or di-lithium salts of carboranes (*ortho*-, *meta*- or *para*-carborane, as appropriate) may react with different carbon-based scaffolds. When the monoalkylation cannot be controlled or heterodisubstituted-carboranes are to be obtained, protection via silylating agents was usually employed.[91] Table 1 presents a summary of the main reactions carried out on the $C_{cluster}$.

2.3.2. Carbaborynes

A powerful synthetic approach that facilitates the synthesis of a wide range of di-C-functionalized *ortho*-carboranes involves the preparation of 1,2-dehydro-*o*-carborane (*o*-carboryne), that is capable of engaging in pericyclic reactions and C–H bond insertions. Based on theoretical studies, *o*-carboryne's energy level is roughly equivalent to that of benzyne, measuring around –99 kcal mol^{-1}. Additionally, the difference in energy between the lowest unoccupied molecular orbital (LUMO) of *o*-carboryne and the highest occupied molecular orbital (HOMO of butadiene, or $E(_{LUMOene-HOMOdiene})$, is less than that of ethylene and benzyne.[115] These findings imply that *o*-carboryne and benzyne may have some similarities and can be thought of as a three-dimensional relative. To

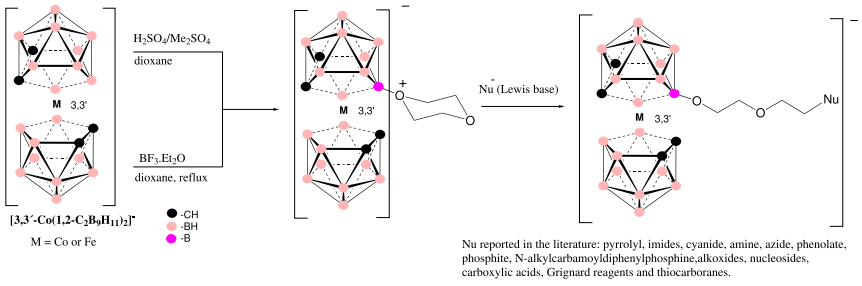

Figure 16. Synthesis of zwitterionic species, followed by the functionalization of B(8/8') vertex by dioxane ring-opening by nucleophiles.[80-85,87] For clarity, cluster numbering has been omitted.

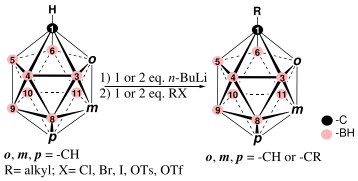

Figure 17. General synthetic procedure for mono- or di-substitution at carbon cluster.

Table 1. Reaction on the carbon of the cluster

Carborane precursor	Product and reference
	Reactions with sp^3-carbon atom
	 92-95 96-100
	Reactions, copper-mediated, with sp^2- or sp-carbon atom
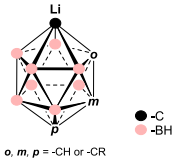	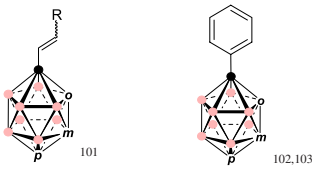 101 102,103
	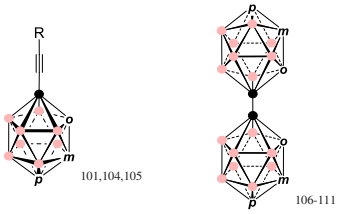 101,104,105 106-111
	Reactions with sp^2-carbonyl carbon atom (CO_2 insertion or salt elimination)
	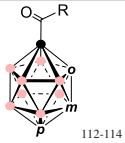 112-114

For clarity, cluster numbering has been omitted.

prepare the *ortho*-carborane for the reaction with π systems, the hydrogen atoms at the cluster carbon atoms must be removed to generate 1,2-dehydro-*ortho*-carborane. The main approaches discussed in the literature are shown in Figure 18.

ortho-Carborynes exhibit remarkable reactivity even at low temperatures. Their reactions can be roughly classified into two groups: C–H bond insertion reactions and pericyclic reactions [4 + 2], [2 + 2] and ene reactions. Table 2 presents a summary of the main reactions carried out from *ortho*-carboryne. The following references provide substantial documentation of the investigation into the chemistry of carborynes.[116,117]

Recently, novel synthetic methodologies exploiting homolysis reactions within boron clusters, encompassing radical pathways at both the –CH and –BH levels (the latter to be discussed subsequently), have been established. The exploration of innovative synthetic strategies involving B- and C-centered radicals presents a formidable challenge and provides avenues for the functionalization of carborane cages through pathways orthogonal to classical closed-shell reactions. This diversification enhances the array of protocols available for the synthesis of substituted carboranes. Given this situation, light-mediated transformations have received much attention in recent years offering alternative avenues for the generation of functionalized molecules under mild reaction conditions, characterized by high functional group tolerance. On top of all that, visible light facilitates the controlled execution of radical-mediated pathways. Even though photochemistry has a great deal of promise for use in carborane reactions, only few examples have been documented to far.[118,119] Some radical-mediated functionalization processes of carboranes at the CH vertex level are shown in Table 3.

2.3.3. Boron substitutions

Because adding functional groups to the boron atoms in the carborane cage is more challenging, the chemistry of boron-substituted carboranes is less established than that of their carbon-substituted counterparts. The following intrinsic features make the effective and selective B–H functionalization of carboranes a synthetic challenge: (*i*) the elevated B–H bond dissociation energies (BDEs) of carboranes (calculated at 96.5-101.7 kcal mol^{-1}), notably surpassing those of extensively studied Lewis base-stabilized boranes (Figure 19) and; (*ii*) the existence of 10 B–H bonds in a similar chemical environment, which possess difficulties for regioselectivity.

Additionally, the reactivity of the BH vertices will depend on their position and the isomer. Due to their low electron density, boron atoms attached to two carbon atoms (such as B3/B6 in *ortho*-carborane) will exhibit a slight electron attraction. In contrast, boron atoms bonded to a single carbon atom will almost never exhibit this effect, and in the case of boron atoms antipodal to the carbons (such as B9/B12 in *ortho*-carborane), they may exhibit an electro-donation effect. As a result, different kinds of reactions can occur in any part of the carborane cluster, particularly in *ortho*- and *meta*-carborane due to their asymmetry.[125]

Electrophilic substitution or halogenation followed by metal-catalyzed cross-coupling at B–X (X = Br or I) (e.g., Kumada- and Neigishi-type reaction)[126,127] is

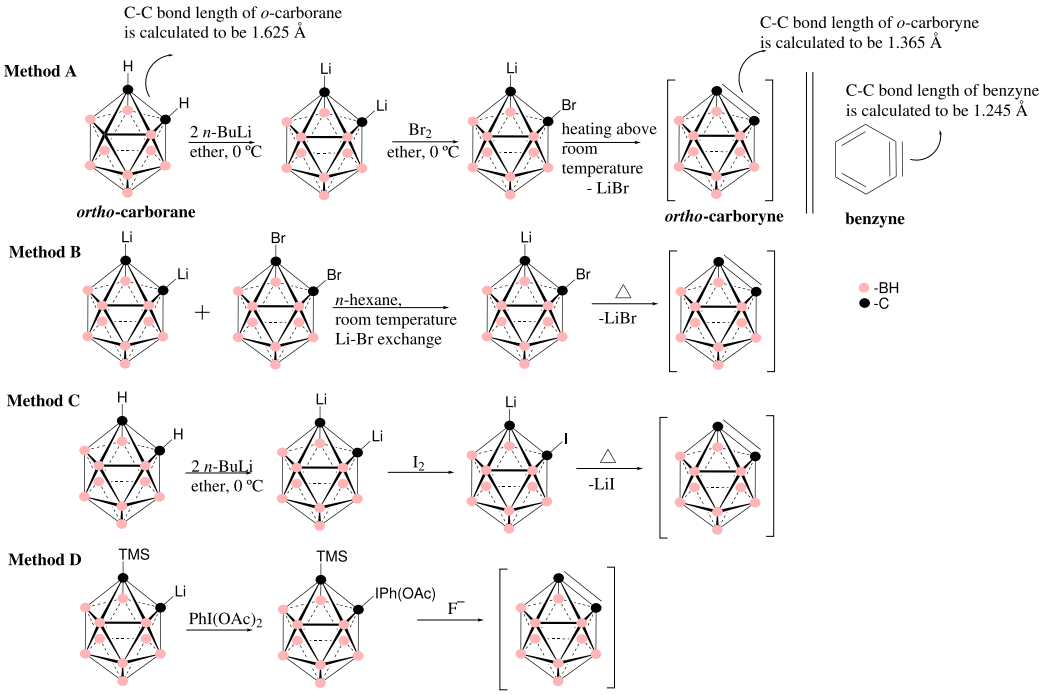

Figure 18. Reported methods for the generation of *ortho*-carboryne. For clarity, cluster numbering has been omitted.

the conventional method for modifying B–H vertex (Figure 20).[39,128,129]

Accordingly, cage B(9,12)–H bonds are the preferred site for Lewis acid-mediated electrophilic halogenation or alkylation, whereas the most electron-deficient B(3,6)–H bonds are not susceptible to electrophilic replacement. Because of this, the synthesis of B(3)-substituted *o*-carborane derivatives is typically accomplished indirectly by deborating ortho-carborane and then reacting the resulting dicarbollide with boron halides in a capitation reaction (Figure 21).

However, the limitations of such approaches include vertex selection and the degree of substitution due to the high cluster symmetry. Transition metal-mediated B–H activation emerges as an enticing alternative to address synthetic challenges in the production of icosahedral carborane and borane derivatives. This method demonstrates the capability to selectively yield desired products with a reduced number of synthetic steps. The underlying strategy is governed by three principles: (*i*) electron-rich transition metal catalysts are deemed suitable for the functionalization of the most electron-deficient B(3,6)H bonds (those bonded to both cage carbons); (*ii*) electrophilic transition metal catalysts are applied for the functionalization of electron-rich B(8,9,10,12)–H bonds (those not bonded to any cage carbons); and (*iii*) a synergistic combination of directing groups with electrophilic transition metal catalysts becomes imperative for B(4,5,7,11)H functionalization (those bonded to only one cage carbon) (Figure 22). Table 4 lists the principal functionalization reactions for each boron vertex along with the corresponding references. As previously discussed, there is a growing interest in selective functionalization at the carbon-cluster through radical processes. This trend is similarly observed in regioselective functionalization of the boron vertices, initiated primarily through light irradiation or photocatalysts. Table 5 shows examples of light-induced selective reactivity at the boron vertices of these boron-rich icosahedral cages.

2.4. Characterization of carboranyl compounds

Carboranes and their derivatives are frequently characterized using standard methods such as X-ray crystallography, infrared (IR) spectroscopy, mass spectrometry (MS), ^{1}H and ^{11}B nuclear magnetic resonance (NMR). The details of carborane characterization have been thoroughly covered by a number of expert reviews,[125,157] thus just the essentials are covered here.

When it comes to ^{1}H NMR spectra of carboranes, the broad signal that appears from 3.00 to ca. 1.3 ppm is always the result of the hydrogen nuclei that are bound to the boron atoms within the cage. Furthermore, the CH protons normally emerge between 2 and 3.5 ppm and are frequently slightly broadened. These latter are most deshielded at 3.55 ppm for *ortho*-carborane and less at 2.91 and 2.75 ppm for *meta*- and *para*-carborane,

Table 2. Reactions with *ortho*-carboryne as starting material

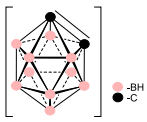

[4 + 2] Diels-Alder reactions

Reactant	Main product
	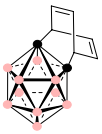
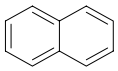	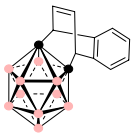
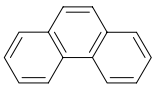	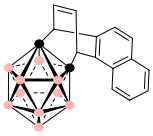

[2 + 2] Cycloaddition reactions

Reactant	Main product
	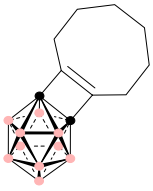
	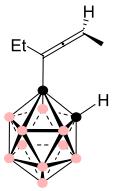

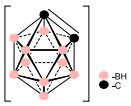

[2 + 2] Cycloaddition reactions

Reactant	Main product
	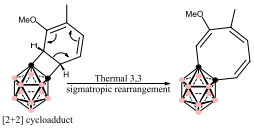
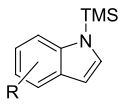 R= alkyl indoles	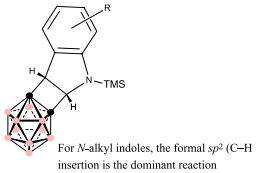 For *N*-alkyl indoles, the formal sp^2 (C–H insertion is the dominant reaction pathway (see below)

Ene reactions

Reactant	Main product
	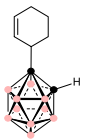

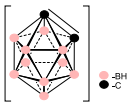

Ene reactions

Reactant	Main product
	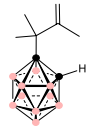
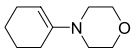	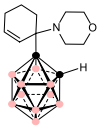
	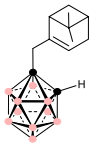

sp^3 and sp^2 C–H bond insertion reactions

Reactant	Main product
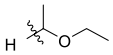	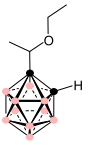
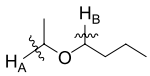 H_A:H_B = 1.1:1	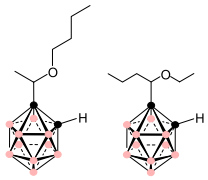

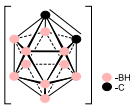

	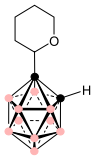
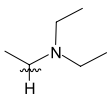	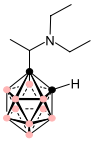
	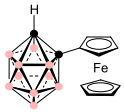
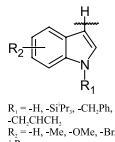 R_1 = -H, -SiⁱPr$_3$, -CH$_2$Ph, -Me, -CH$_2$CHCH$_2$ R_2 = -H, -Me, -OMe, -Br, -F, Cl, *i*-Pr	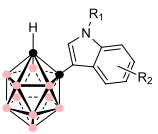

For clarity, cluster numbering has been omitted.

Table 3. Radical-mediated functionalizations at the CH carboranes vertex

Carborane precursor	Reactant and conditions	Main product and reference
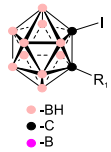	 (hetero)arenes such as furans and pyrroles Na_2CO_3 (1.2 equiv.), DCM, 24 h, UV (18 W) R_1= H, alkyl, allyl, phenyl, benzyl	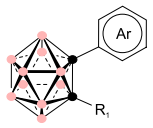 120
	Na_2CO_3 (1.2 equiv.) DCM, 48 h, UV (18 W) 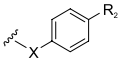 X= O, S, CH_2, HC=CH, $Si(CH_3)_2$	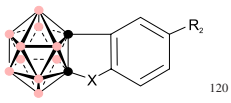 120
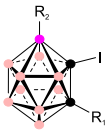	 R_1= CH_3; R_2= H; R_3= *n*Pr, *n*Bu, *n*Pn, Ph, TMS, and others 2,6-lutidine, DCM, 48 h, 36 W, UV (365 nm)	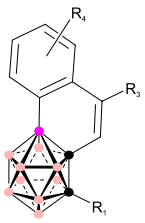 121 this process involves the functionalization at the level of the vertices -C(1) and -B(3)
	 R_1= CH_3; R_2= H; R_3= Ph, PhI, PhCl, PhF, $PhCF_3$, PhEt, Ph*t*-BuO, PhOMe, and others $NaHCO_3$, DCM, 36-48 h, 125 W, UV (365 nm)	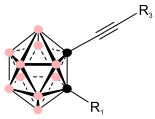 121
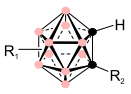 R_1=R_2=H, CH_3	 CuI, *t*-BuOLi, DME, Ag_2CO_3, room temperature, 24 h, 8 W, UV (254 nm)	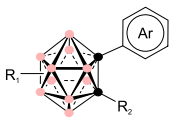 122
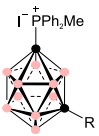	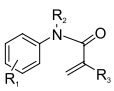 *N*-arylacrylamides, KOAc (2 equiv.) DCM, 36 h, 45 ºC, blue light-emitting diode (LED) R_1, R_2 and R_3 are more precisely detailed in the referenced document	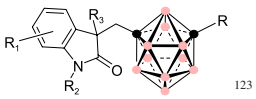 123

For clarity, cluster numbering has been omitted. DCM: dichloromethane.

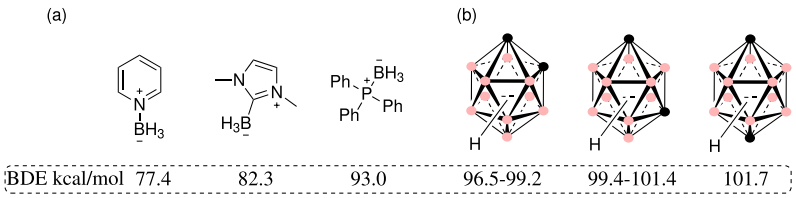

Figure 19. B–H bond dissociation energies (BDE) of representative boranes. (a) Examples of ligand boranes and (b) icosahedral carboranes.[124]

respectively, setting the *ortho* isomer apart from the other two (Figure 23). For *nido*-carborane derivatives, the bridging hydride gives rise to a distinctive doublet between −2.5 and −3.0 ppm (spectrum not shown). Regarding B–NMR, it is important to consider that both ^{10}B (with spin quantum number, I = 3) and ^{11}B (I = 3/2) are active nuclei in NMR. However, the latter isotope, constituting 80.3% of natural boron, is more frequently employed in NMR experiments. This preference is attributed to its high abundance, relatively elevated receptivity (10% of ^{1}H), reasonable peak width at half-height, and short average relaxation times.[158] In the $^{11}B\{^{1}H\}$ spectra (Figure 24), the boron atoms in the *para*-carborane exhibit uniform chemical shifts, with

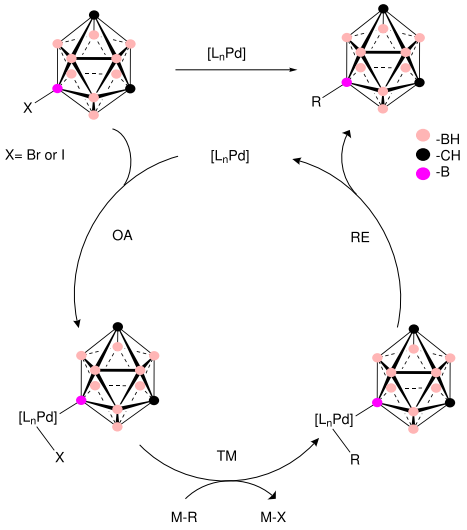

Figure 20. A representative halocarborane's generalized Pd-catalyzed cross-coupling, in which the halogen is bonded to the B(9) position of a meta-carborane cluster. TM stands for transmetallation, RE for reductive elimination and OA for oxidative addition. For clarity, cluster numbering has been omitted.

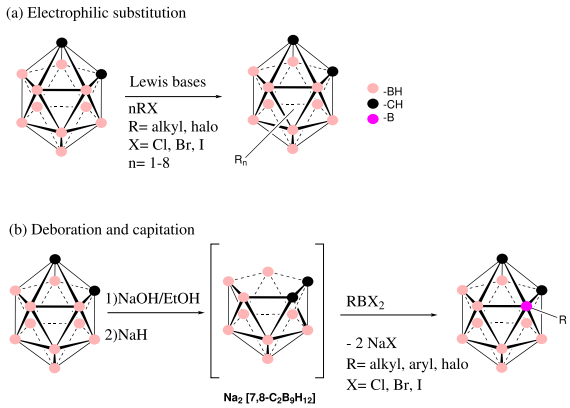

Figure 21. (a) Electrophilic substitution of *ortho*-carborane and cage-reconstruction of *ortho*-carborane by deboronation and subsequent "recapitation" (b). For clarity, cluster numbering has been omitted.

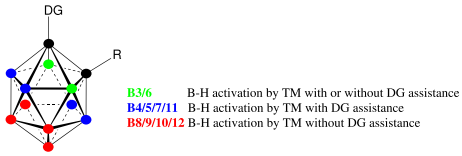

Figure 22. General strategy for catalytic selective cage B–H activation strategies of *ortho*-carboranes. DG, directing group; TM, transition metal.

values of roughly −14.8 ppm (Figure 24). On the other hand, the boron atoms in the *ortho*- and *meta*-carborane display four different sets in a 2:2:4:2 ratios. The chemical shifts for *meta*-carborane are −6.7, −10.5, −13.3, and −17.0 ppm, and for *ortho*-carborane they are −2.5, −9.3, −13.6, and −14.7 ppm. The opposite vertices, which are the most deshielded, suffer an antipodal influence from the boron atoms that are nearest to the carbon atoms, which are the most protected. Furthermore, electron density and symmetry are commonly altered by the addition of substituents at various cluster locations, and this may affect signal count through signal overlap and broadening. As a result of coupling with the terminal hydrogen atoms (*exo* BH bond), the boron multiplicity splits into doublets. Depending on the substituents, the $^{1}J_{BH}$ coupling constants for the unsubstituted isomers range from 150 to 180 Hz (Figure 24), whereas for the substituted isomers they are roughly 120-210 Hz. Deboronation yields a readily identifiable cluster anion (the *nido*-carborane) and resonances in ca. 5 to 40 ppm range (spectra not depicted). According to the ^{13}C NMR spectra obtained in $CDCl_3$, *ortho*-carborane shows a singular resonance at 54.5 ppm ($^{1}J_{CH}$ 193 Hz), *meta*-carborane shows a peak at 55.2 ppm ($^{1}J_{CH}$ 179 Hz), and *para*-carborane shows the most deshielded appearance at 63.5 ppm ($^{1}J_{CH}$ 180 Hz). The introduction of an organic substituent at a $C_{cluster}$ atom induces deshielding in the corresponding cluster carbon atom and the adjacent polyhedral carbon atom. The degree of this deshielding action varies depending on the kind of substituent and is most noticeable in *ortho*-carborane (*ortho* effect).[159] Deboronation to the anionic *nido*-carboranes leads to shielding of the cluster carbon atoms and yields broad signal.[160]

Regarding the IR spectroscopy is a useful tool for characterizing carborane derivatives. The broad B–H stretching band, which does not overlap with other typical organic vibrational bands, is extremely characteristic of carboranes and is found at 2603, 2605, and 2612 cm^{-1} (for *ortho*-, *meta*- and *para*-isomer, respectively). Moreover, *nido*-carboranes exhibit this band at wavenumbers below 2600 cm^{-1}. The order in which the stretching vibrations $\nu_{(CH)}$ decrease is *ortho*- > *meta*- > *para*-carbaborane (3070, 3064, 3060 cm^{-1}). For all isomers, the $\nu_{(BB)}$ vibration at roughly 720 cm^{-1} represents the "pulsation" of the cage (antisymmetric cage stretching vibration).[161] Some isomer displays an extra unique fingerprint at 1250-1150 cm^{-1} and 1050-980 cm^{-1} that corresponds to the CH and B–H bending (δ) vibrations respectively. However, it is pertinent to note that, a difference between *ortho*- and *meta*-carborane derivatives occurs in their $\delta_{(C\text{-}H)}$ bands where the 1220 cm^{-1} band is only seen in *ortho*-carborane and its derivatives.

As previously mentioned, there are two naturally occurring isotopes of boron, ^{10}B and ^{11}B, with an isotopic distribution of (^{10}B/^{11}B = 2/8). As a result, carboranes produce a particularly distinctive pattern in mass spectra (Figure 25).[162] The *ortho*-carborane mass spectrum displays an isotope distribution between *m/z* 136 and 146 with a base peak of *m/z* 144 (M^+ or M^-), which corresponds to $^{12}C_{21}H_{12}{}^{10}B_2{}^{11}B_8$. Due to the presence

Table 4. Functionalizations at the BH carboranes vertex

Carborane precursor	Reactant and condition	Main product and reference
Transition metal-catalyzed selective cage B(3,6)-H functionalization		
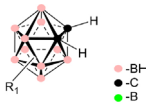 R_1= H, I, alkyl, alkenyl, aryl and benzyl	$[(COD)IrCl]_2$ (3.5 mol%), 2-MePy (21 mol%), B_2pin_2 (4 equiv.), THF, 110 °C, 5 h	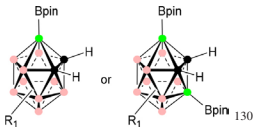 130
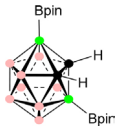	PhBr (3 equiv.), $Pd(PPh_3)_4$, (20 mol%), Cs_2CO_3 (3 equiv.), cyclohexane, 150 °C (bath), 8 h	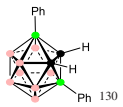 130
	allyl chloride (6 equiv.), $Pd(dba)_2$ (20 mol%), Cs_2CO_3 (3 equiv.), toluene, room temperature, 24 h	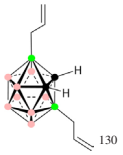 130
	PhX (3 equiv.), $Pd(PPh_3)_4$, (10 mol%), *t*-BuOK, (3 equiv.), THF, 80 °C, 24 h	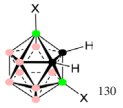 130
	$Cu(OAc)_2$ (6 equiv.), KF (6 equiv.), CH_3CN, 80 °C, 12 h, under O_2 (1 atm)	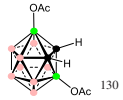 130
	MeONHLi, THF, 80 °C, 8 h	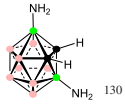 130
	$TMSN_3$ (2.4 equiv.), CuCl (2.1 equiv.), KF (2.4 equiv.), THF, 60 °C, 24 h	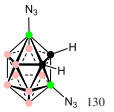 130
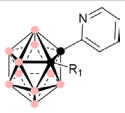 R_1= H, Me and Bn	5 mol% $[Cp^*RhCl_2]_2$, AgOAc (20 mol%) R_2COOH (6 equiv.), $Cu(OH)_2$ (3 equiv) oxone (2 equiv.), DCE, 120 °C, 24 h	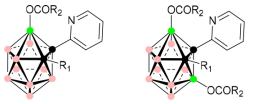 R_2= alkyl, phenyl, thienyl and indolyl 131
	$Pd(OAc)_2$ (10 mol%), IPrHCl (20 mol%) ArI (4 equiv.), Ag_2CO_3 (2 equiv) Et_2O, 25 °C, 24 h	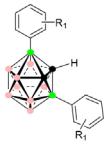 R_1 = H, halo, CF_3, CHO and COOEt unsymmetrical B(3,6)-diarylated *ortho*-carboranes could be prepared when employing 3-phenyl-*o*-carborane as a substrate 132
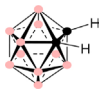	$[Cp^*IrCl_2]_2$ (8 mol%) ≡—Alk (6 equiv.) PhCOOH (1 equiv.) 1,4-dioxane 130 °C, 18 h	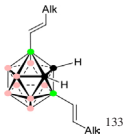 133
	$[Cp^*IrCl_2]_2$ (4 mol%) ≡—Alk (1.5 equiv.) 1,4-dioxane 70 °C, 12 h	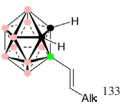 133
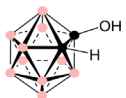	Pd(OAc)2 (10 mol%) Ar—≡—Ar (2 equiv.) $PhI(OAc)_2$ 2 (equiv.) CH_3CN, 25 °C, 12 h	 Ar = $R_1C_6H_4$, thienyl, naphthyl and furanyl R_1= H, MeO, alkyl, halo, CF_3, MeCO and MeOCO 134

Table 4. Functionalizations at the BH carboranes vertex (cont.)

Carborane precursor	Reactant and condition	Main product and reference
Transition metal-catalyzed selective cage B(4,5,7,11)-H functionalization		
 R_1 = H, Me and Bn Ar = $R_5C_6H_4$ and thienyl R_5 = H, alkyl, halo, CF_3, MeO, MeS and MeOCO COOH as a guiding group to achieve Ir-catalyzed B(4)-alkenylation	$[Cp^*IrCl_2]_2$ (2.5 mol%) Ar—≡—Ar (1.2 equiv.) $Cu(OAc)_2$ (0.5 equiv.) AgOAc (0.5 equiv.) toluene, 130 °C, 18 h	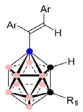
 R_1 = H, alkyl, Bn and TMS Ar = $R_5C_6H_4$ and naphthyl R_2 = H, alkyl, halo, CF_3 and MeO COOH as a guiding group	$Pd(OAc)_2$ (10 mol%) $(CH_2{=}CH)Ar$ (2.2 equiv.) AgOAc (4 equiv.) DCE, 50 °C, 12 h	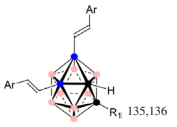 135,136
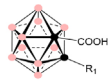 R_1 = alkyl, aryl and Bn COOH as a guiding group	$Pd(TFA)_2$ (10 mol%) $(CH_2{=}CH)COR_2$ (2.2 equiv.) AgOAc (4 equiv.) DCE, 70 °C, 18 h R_2 = *t*-Bu, aryl and amino	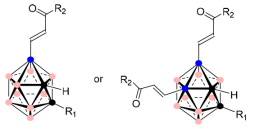 R_2 = *t*-Bu, aryl and amino or R_2 = OR_3, R_3 = alky, Bn and Ph 137
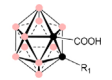 R_1 = H, Me, Ph, Bn and TMS Ar = $R_5C_6H_4$ and naphthyl R_2 = H, alkyl, halo, acyl, MeOCO, Ph and MeO COOH as a guiding group	$Pd(OAc)_2$ (10 mol%) ArI (3 equiv.) AgOAc (3 equiv.) AcOH (5 equiv.) toluene, 70 °C, 12 h	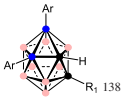 138
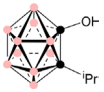	$Pd(OAc)_2$ (10 mol%) R_2—≡—R_1 (2 equiv.) CO (1 atm.) $(iPr)_2S$ (1 equiv.) MesCOOH (25 mol%) $Cu(OAc)_2$ (0.5 equiv.) Ag_2CO_3 (1.5 equiv.) toluene, 160 °C, 3 h	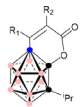 R_1 = $R_3C_6H_4$, thienyl, naphthyl and alkyl R_2 = $R_3C_6H_4$, thienyl and naphthyl R_3 = H, alkyl, halo, CF_3, MeO, MeS and TMS 139
	$Cu(OTf)_2$ (20 mol%) 2-PhPy (20 mol%) R_2—≡—R_3 (2 equiv.) Ag_2CO_3 (2 equiv.) Li_2CO_3 (2 equiv.) DCE, 130 °C, 12 h	 140
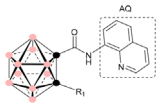 R_1 = alkyl R_2, R_3 = (hetero)aryl, alkyl, alkynyl and COOMe R_4 = (hetero)aryl COOH as a bidentate directing group to achieve B(4)-substitution	$Cu(OTf)_2$ (2 equiv.) 2-PhPy (2 equiv.) H—≡—R_4 (2 equiv.) Ag_2CO_3 (2 equiv.) K_2HPO_4 (2 equiv.) DCE, 130 °C, 12 h	 140
as a transient directing group guided  R_1 = alkyl, aryl and benzyl Ar = $R_2C_6H_4$ and naphthyl	$Pd(OAc)_2$ (10 mol%) ArI (3 equiv.) AgTFA (2 equiv.) TFA (1 equiv.) HFIP, 80°C, 36 h	 R_3 = H, alkyl, halo, acyl, MeOCO, Ph, NO_2, MeO and AcHN
	$Pd(OAc)_2$ (5 mol%) ArI (1.2 equiv.) AgTFA (1.2 equiv.) TFA (1 equiv.) HFIP, 60°C, 24 h	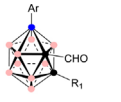 R_2 = alkyl, halo, acyl, MeOCO, CN, MeO and NO_2 141

Table 4. Functionalizations at the BH carboranes vertex (cont.)

Carborane precursor	Reactant and condition	Main product and reference
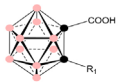 R_1 = H, alkyl and benzyl thiophenes, benzothiophenes, thienothiophenes and oligothiophenes COOH as a guiding group	benzothiophenes, thienothiophenes and oligothiophenes  $[Cp^*IrCl_2]_2$ (5 mol%) $AgNTf_2$ (10 mol%) AgOAc (10%) Li_2CO_3 (2 equiv.) $Cu(OAc)_2$ (3 equiv.) toluene, 130 °C, 24 h	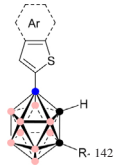 R- 142
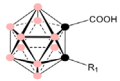 R_1 = alkyl, aryl, benzyl, alkenyl and TMS COOH as a guiding group	$Pd(OAc)_2$ (5 mol%) R_2—≡—Br (1 equiv.) AgOAc (3 equiv.) DCE, 90 °C, 6 h	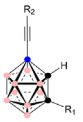 R_2 = *i*-Pr_3Si and *t*-$BuMe_2Si$ 143
	$Pd(OAc)_2$ (5 mol%) R_2—≡—H (2 equiv.) AgOAc (3 equiv.) K_2HPO_4 (2 equiv.) DCE, 90 °C, 6 h	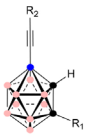 R_2 = silyl, aryl and carboranyl 143
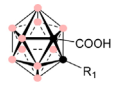 R_1 = alkyl and Ph COOH as a guiding group	$[Cp^*RhCl_2]_2$ (5 mol%)  R_2 (2.4 equiv.) AgOAC (4 equiv.) 1,4-dioxane, 70 °C, 18 h R_2 = alkyl and aryl	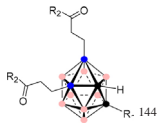 R- 144
B(9)-acyl amino group guided Pd-catalyzed B(4)-methylation 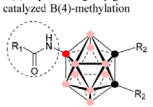 R_1 = $R_3C_6H_4$, R_3 = alkyl, MeO, F, Cl, CF_3 R_2 = H, alkyl	$Pd(MeCN)_4(Cl)_2$ 10 (mol%) MeI (2 equiv.) AgOAC (3 equiv.) toluene, 25 °C, 12 h	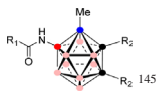 145
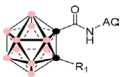	RVC | Pt Cu(OTf)$_2$ (50 mol%) LiOAr (8 equiv.) LiO*t*-Bu (2 equiv.) *n*Bu_4NOTf (0.375 M) 4 mA, THF, 25 °C,12 h R_1 = *i*-Pr	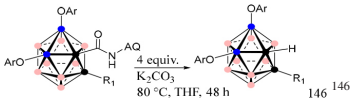 146 146
	RVC | Pt Cu(OTf)$_2$ (50 mol%) LiO*t*-Bu (5 equiv.) *n*Bu_4NOTf (0.25 M) 4 mA, THF, 25 °C,12 h R_1 = alkyl and phenyl	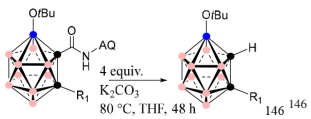 146 146
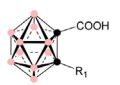 R_1 = H, alkyl, benzyl, styryl and TMS COOH as a guiding group	$[Ru(p\text{-cymene})Cl_2]_2$ (2.5 mol%) N_3-R_3 (1.1 equiv.) R_3 = sulfonyl NaOAc (2 equiv.) toluene, 100 °C, 12 h	 147

Table 4. Functionalizations at the BH carboranes vertex (cont.)

Carborane precursor	Reactant and condition	Main product and reference
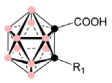 R_1 = H, alkyl, benzyl, styryl and TMS COOH as a guiding group	$Pd(OAc)_2$ (10 mol%) $BzO-(NR_2)_2$ (1.2 equiv.) K_2HPO_4 (1 equiv.) toluene, 100 °C,12 h R_2 = alkyl and benzyl	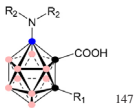 147
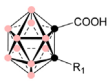 R_1 = H, alkyl, benzyl, styryl and TMS COOH as a guiding group	$Pd(OAc)_2$ (15 mol%) IOAc (2 equiv.) NaOAc (1 equiv.) toluene, 60 °C, 6 h	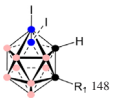 148
	$[Cp^*IrCl_2]_2$ (2.5 mol%) halogenating source: NIS (1 equiv.) for I; NBS (1 equiv.) for Br $FeCl_3$ and $Cu(OAc)_2$ (2 equiv.) for Cl $AgNTf_2$ (10 mol%) NaOAc (1 equiv.) DCE, 100-120 °C, 12 h	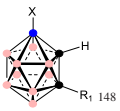 148
 R_1 = alkyl, phenyl and benzyl R_2 = $R_3C_6H_4$, naphthyl, thienyl, furanyl and alkyl; R_3 = alkyl, halo, OMe, SMe and CF_3	$Cu(OTf)_2$ (1 equiv.) R_2-S-SR_2 (3 equiv.) 2PhPy (1 equiv.) Li*O*-*t*-Bu (4 equiv.) DCE, 130 °C, 48 h	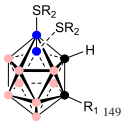 149
Transition metal-catalyzed selective cage B(8,9,10,12)-H functionalization		
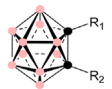 R_1, R_2 = H, alkyl, alkenyl, aryl and benzyl	$Pd(MeCN)_4(BF_4)_2$ (0.5 equiv.)  (10 equiv.) MeCN, 110 °C	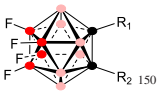 150
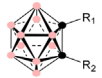 R_1, R_2 = alkyl, aryl and benzyl	$Pd(OAc)_2$ (2 mol%) $FeCl_3$ (2 equiv.) AcOH, 80° C, 6-24 h	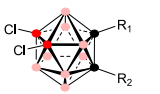 B(8):B(9) = ~1:1 151
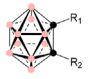 R_1, R_2 = alkyl, aryl and benzyl R_3 = aryl, naphthyl, acyl and esteryl	$Pd(OAc)_2$ (10 mol%) CH_2=CHR_3 (2 equiv.) AgOAc (2 equiv.) THF, 80° C, 48 h	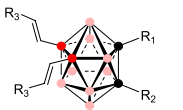 B(8):B(9) = ~1:1 152
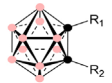 R_1, R_2 = H, alkyl and benzyl Ar = $R_3C_6H_4$; R_3 = H, alkyl, alkoxyl, halo, esteryl and acyl	$Pd(OAc)_2$ (10 mol%) ArI (3 equiv.) Ag_2CO_3 (2 equiv.) DCE, 60° C, 48 h	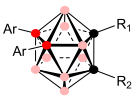 B(8):B(9) = 1:1.4 - 1:2.7 153
	$Pd(OAc)_2$ (10 mol%) $PhI(OAc)_2$ (2 equiv.) AgOAc (1 equiv.) DCM/AcOH (1:1), 40° C, 24-36 h	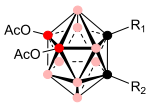 B(8):B(9) = ~1:1
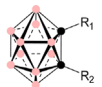 R_1, R_2 = alkyl, alkenyl, benzyl and aryl	$Pd(OAc)_2$ (2 mol%) $PhI(OAc)_2$ (8 equiv.) AcOH/Ac_2O (1:1), 100 °C, 12-24 h	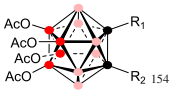 154

For clarity, cluster numbering has been omitted. THF: tetrahydrofuran; DCE: 1,2-dichloroethane; NIS: *N*-iodosuccinimide; NBS: *N*-bromosuccinimide; ArI: iodobenzene; AgTFA: trifluoroacetic acid silver salt; TFA: trifluoroacetic acid; HFIP: 1,1,1,3,3,3-hexafluoro-2-propanol; RVC: reticulated vitreous carbon.

Table 5. Light-induced functionalizations at the BH carboranes vertex

Carborane precursor	Reactant and conditions	Main product
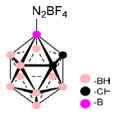	 eosin Y (2 mol%) MeCN, room temperature, 2 h, 530 nm (12 W)	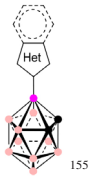 155
 3-, 4-, 9-iodo and 9,12-diiodo *ortho*-carborane	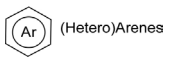 $Pd_2(dba)_3$ $P(4\text{-}F\text{-}C_6H_4)_3$ Cs_2CO_3 MeCN, room temperature, 48 h, blue LED (30 W)[122]	
	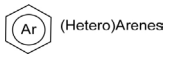 $Ni(PPh_3)_2I_2$ (10 mol%) $P(4\text{-}F\text{-}C_6H_4)_3$ Zn (1 equiv.) Cs_2CO_3 MeCN, room temperature, 48 h, blue LED (30 W)[156]	
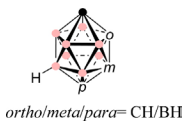 *ortho*/*meta*/*para*= CH/BH	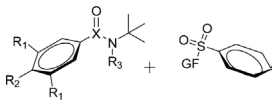 $PhCF_3$ (0.5 M) room temperature, Ar, 12 h, blue LED (12 W) FG: SR/ SePh/ 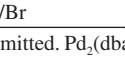 CN/Cl/Br	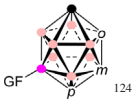 124

For clarity, cluster numbering has been omitted. $Pd_2(dba)_3$: tris(dibenzylideneacetone)dipalladium(0).

of the carbon isotope ^{13}C, which has a 1.1% natural abundance in carbon, there are also small peaks of *m/z* 147 and 148.[157]

3. Medicinal Chemistry of Polyhedral Boron Clusters

3.1. Medicinal chemistry of PBC not BNCT related

The PBC have been used as a potential component of other chemotherapeutics, despite its significant utility in BNCT.[163] Some of the most recent PBC applications will be briefly covered.

New PBC-derived compounds that have the ability to inhibit cyclooxygenase-2 (COX-2) have recently been reported for use as anti-inflammatory, analgesic and anti-pyretic drugs.[163] Moreover, inflammatory conditions like rheumatoid arthritis, neurological conditions like Alzheimer's disease, and numerous cancer types are linked to COX-2 overexpression. The PBC carboranes were proposed as phenyl-mimetics, for their three-dimensional aromaticity, and due to their low toxicity, high hydrophobicity, and metabolic stability, this system was selected to prepare different kind of compounds. In this sense, the bulky 2,6-di-*tert*-butyl-1-hydroxyphenyl COX-2/5-lipoxygenase (5-LO)-inhibition pharmacophore was substituted by 1-hydroxy-1,2-carboran-12-yl motif generating new derivatives like MedChem_1 (Figure 26) with potent anti-5-LO activity and low cytotoxic potential.[164]

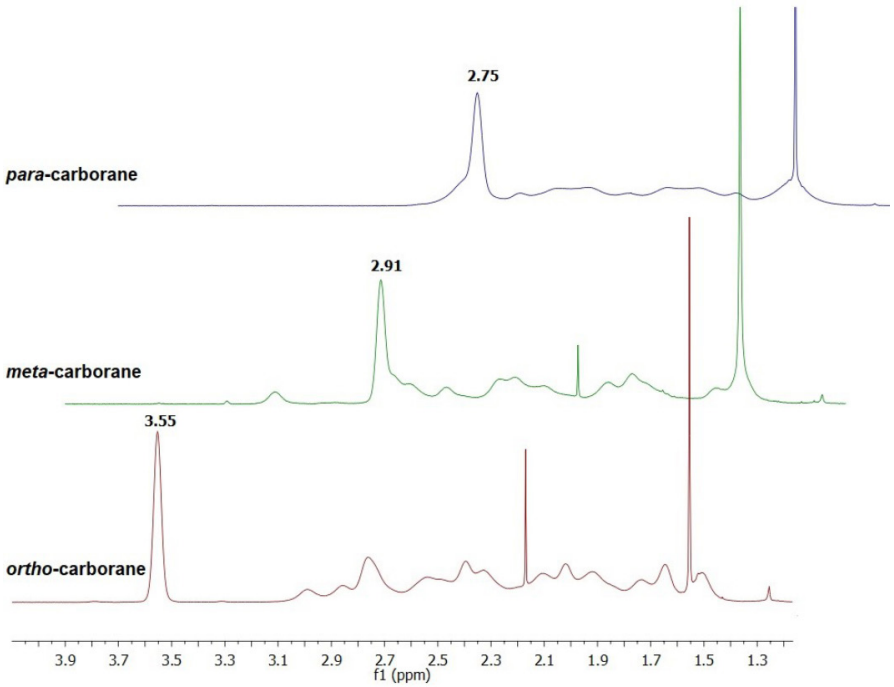

Figure 23. ^1H NMR spectra (400.13 MHz, $CDCl_3$) of unsubstituted carboranes commercially available.

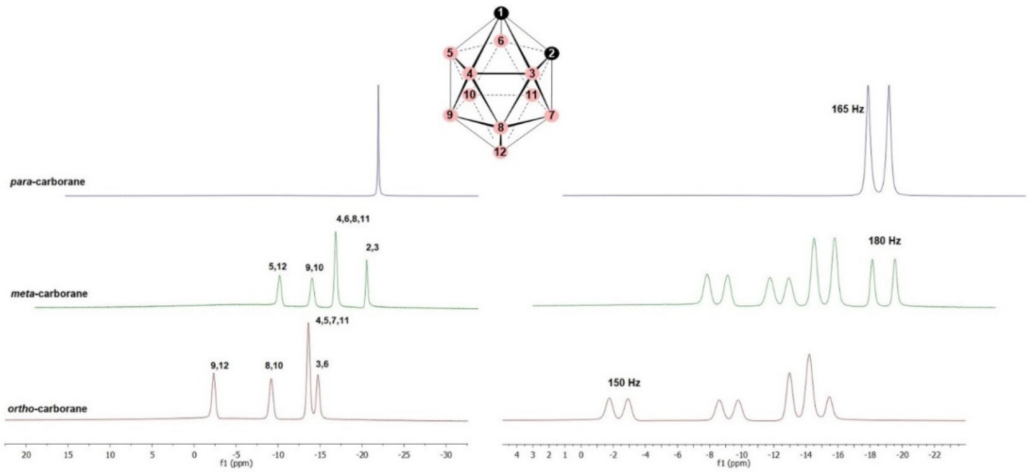

Figure 24. The ^{11}B NMR spectra (128.38 MHz, $CDCl_3$) of commercially available unsubstituted carboranes and labeled with the corresponding positions of the boron atoms. The spectra are shown as proton-decoupled (left) and proton-coupled (right). Selected $^1J_{BH}$ coupling constants are also provided.

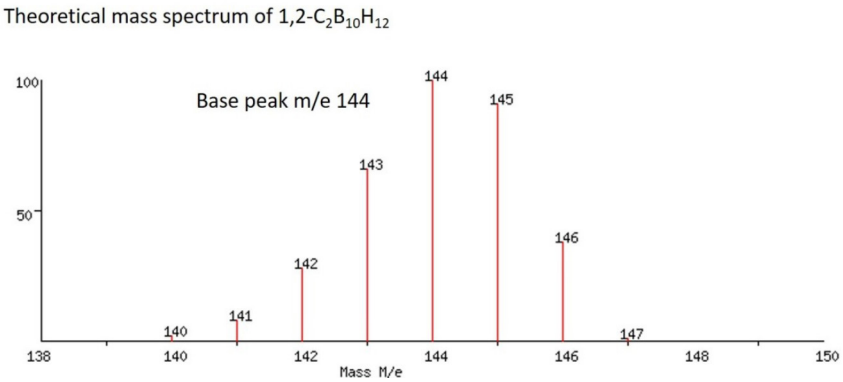

Figure 25. Predicted using simulator.[162]

Similarly, the electron-deficient half-sandwich iridium complex [Ir(η5-pentamethylcyclopentadiene)(1,2-dicarba-closo-dodecarborane-1,2-dithiolato)] (MedChem_2, Figure 26) triggers, like the phenyl-bioisoster [Ir(η5-penta methylcyclopentadiene)(benzene-1,2-dithiolato)], a full anti-inflammatory response against lipopolysaccharides-induced NO production without cytotoxic effects.[165]

A significant amount of work has gone into creating photosensitive drugs for anticancer treatment, with the porphyrin heterocycle serving as the main pharmacophore due to its special photophysical properties, selectivity for tumor cells and low *in vivo* toxicity. Thinking about dual mechanisms drugs, photodynamic therapy together with BNCT, the PBC have been used in the generation of new kind of compounds. For example,[166] compounds MedChem_3 and MedChem_4 (Figure 26) were synthesized from the common starting material cyanuric chloride (2,4,6-trichloro-1,3,5-triazine) and evaluated for their cytotoxicity in the dark, percentage of HCT116 human colon carcinoma cells survival > 75% at doses less than 50 μM, and after photoactivation, the half maximal inhibitory concentration were $IC_{50,MedChem\_3}$ = 20 μM and $IC_{50,MedChem\_4}$ = 16 μM.

Using as structural-template the 4-anilino-2-pyridylquinazoline pharmacophore for the inhibition of *h*ABCG2 (human breast cancer resistance protein), different PBC-derivatives were developed (MedChem_5, MedChem_6 and MedChem_7, Figure 26) as reverter of the multidrug resistance (MDR) in cancer promoted by the ATP-binding cassette (ABC) transport proteins.[167] MedChem_5 displayed lower inhibitory activity than the reference used in the assay but was able to reverse the ABCG2-based mitoxantrone resistance. MedChem_6 and MedChem_7 exhibited higher solubility and lower toxicity as their phenyl (2D-aromatic bioisoster) and adamantyl (3D-steric bioisoster) analogues and were able to reverse mitoxantrone resistance in MDCKII-hABCG2 and HT29 colon cancer cells. Similar biological behavior was observed with MedChem_8 (Figure 26) a carborane inspired in baicalein, an inhibitor of *h*ABCG2 efflux activity in RPMI8226 cells, having inhibitory effects in nanomolar ranges and producing an increase in mitoxantrone toxicity.[168]

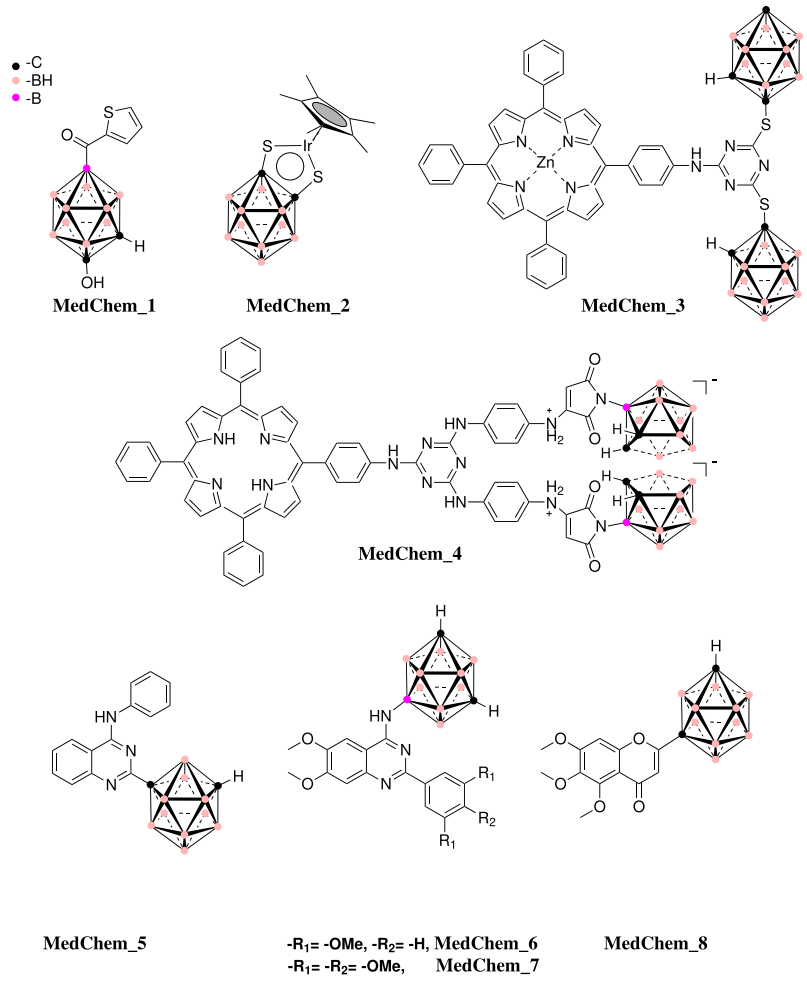

Figure 26. PBC described recently with different medicinal chemistry applications.

3.2. Medicinal chemistry of PBC within BNCT

BNCT has been the primary focus of PBC medicinal chemistry production to date. In 2023, Marforio *et al.*[11] presented a very interesting updated review on the carboranes in BNCT. Table 6 summarizes chemical structures, biological targets and activities, along with the corresponding references, of some of the first approaches, prior to 2022, that have been studied in the generation of PBC for use in BNCT.

In the following lines, the most relevant and current studies in medicinal chemistry of PBC within BNCT will be highlighted.

Among the different strategies used to include PBC into potential BNCT agents has been to incorporate structural fragments with the ability to recognize specific drug transporting biomolecules, specifically albumin. Serum albumin ligands, which can bind to it when injected into the blood, have been used as an additional strategy to prepare new boron-containing compounds that, forming complexes with albumin, reach the tumor and are released there. Recently, the human serum albumin (HSA) non-covalent ligand containing 4-iodophenylbutanoyl-moiety[177] has been used to conjugate with the *closo*-dodecaborate system. For example, PBC_1 (Figure 27) demonstrated low cancer cells toxicity, high interaction with HSA (dissociation constant of 148 μM, three bounded PBC_1s *per* molecule of HSA) and good *in vivo* accumulation in U87 MG tumor mouse model.[178] In a study of BNCT *in vivo*,[179] using F98 glioma-bearing rats, PBC_1 displayed lower survival time than the BNCT with BPA group while showed survival improvement compared to not treated- and neutrons treated-animals. The same research group reported the use of these HSA ligand, 4-iodophenylbutanoyl-moiety, and PBC, *closo*-dodecaborate system, to prepare a new potential agent to BNCT that possesses a folate receptor α (FRα)-targeting framework (PBC_2, Figure 27). FRα plays an important role in embryogenesis, but is not widely expressed after embryogenesis having a minor role in non-malignant cells with overexpression in several solid tumors. The *in vivo* biological behavior of PBC_2, in U87 MG-, F98-, and C6-tumor-bearing animals, was very promising

Table 6. Some of the first approaches, prior to 2022, using PBC with potential use in BNCT

PBC example and reference	Biological target
PBC-conjugated antibodies and antibodies fragments[169]	designed and developed as targeted to antigens differentially expressed in tumor tissues
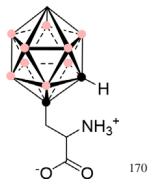 170	designed and developed as phenylalanine bioisoster, like BPA *in vivo* studies ruled out its use for BNCT
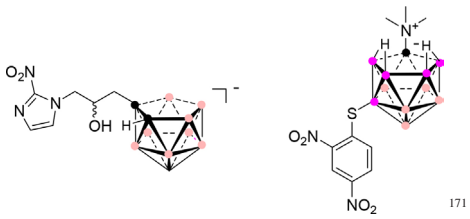 171	designed and developed as BNCT agents that preferentially accumulated in hypoxic tissues after undergo reductive activation
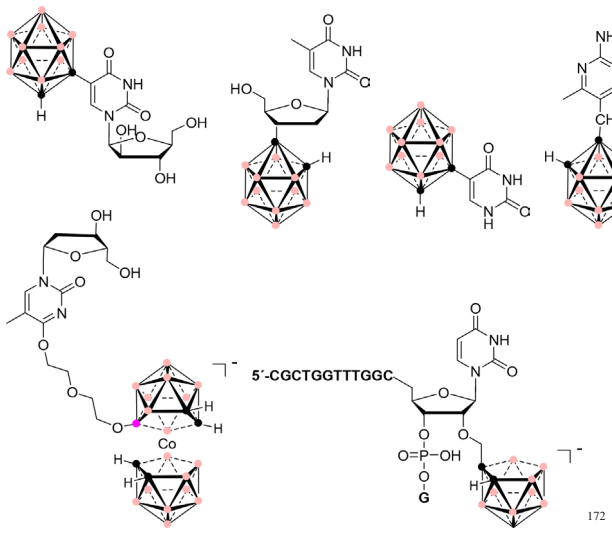 172	designed and developed as agent to be selectively accumulated in rapidly multiplying tumor cells, conversion to the corresponding nucleotides, trapped within the cell and nuclear DNA of tumors incorporation
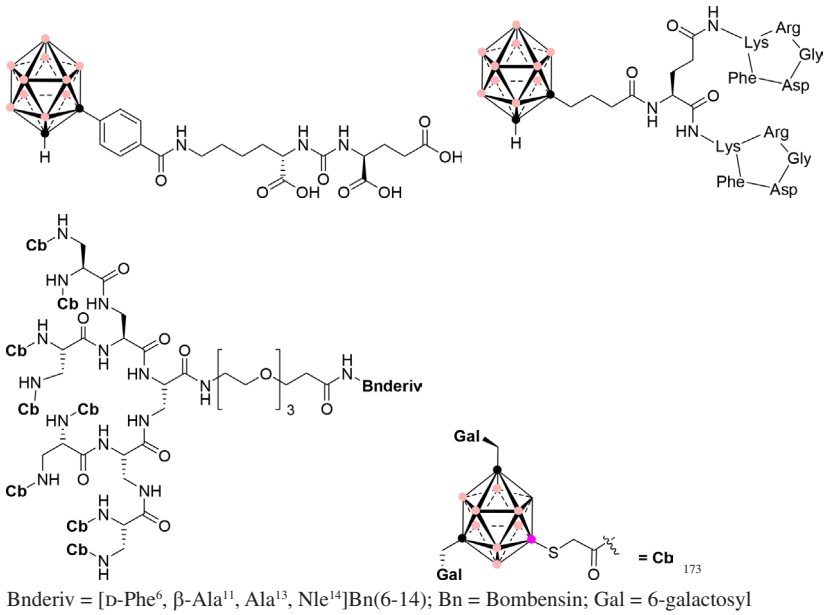 173	designed and developed as agent to recognize and bind to certain receptors, that aminoacidic sequences are able to bind them, present on the surface of cancer cells

Bnderiv = [D-Phe^{6}, β-Ala^{11}, Ala^{13}, Nle^{14}]Bn(6-14); Bn = Bombensin; Gal = 6-galactosyl

Table 6. Some of the first approaches, prior to 2022, using PBC with potential use in BNCT (cont.)

PBC example and reference	Biological target
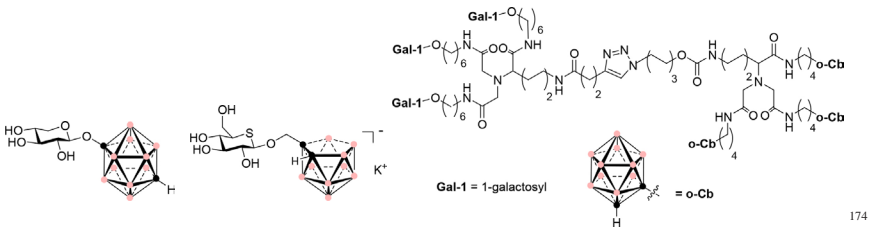 Gal-1 = 1-galactosyl; = o-Cb 174	designed and developed as agents to recognize and bind to certain receptors, that glycosides are able to bind them, or incorporated in some sugars involved-biochemical pathways
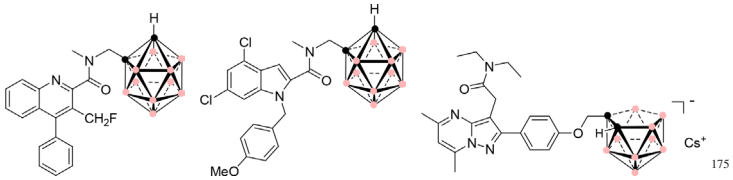 175	designed and developed as agent to bind to trans20240109 protein located in the outer mitochondrial membrane of cells, upregulated in a variety of tumor cell lines
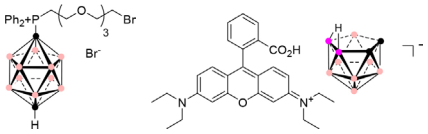 Designed and developed as delocalized lipophilic agents able to accumulate selectively in cancer cells mitochondria	
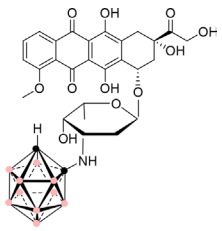 The nuclear translocation property of doxorubicin was used in the design and development of BNCT agents	
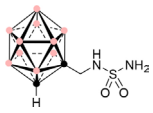 Designed and developed as agent to bind to carbonic anhydrase IX, enzyme that regulates pH in hypoxic regions	designed and developed to bind or interact to other biotargets[176]
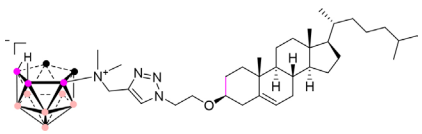 Designed and developed as agent to bind to low-density lipoprotein (LDL) and accumulates in tumor cells with up-regulation of LDL transporters or to prepare liposomes	
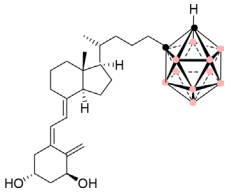 Designed and developed as agent to bind to vitamin D nuclear receptor expressed in tumors	
● -C, ● -BH, ● -B	

PBC: polyhedral boron clusters; DNA: deoxyribonucleic acid; BPA: L-phenylalanine; BNCT: boron neutron capture therapy.

showing: (*i*) better boron accumulation in tumors- and suppressing tumor growth in BNCT-regimens-more than BPA; (*ii*) excellent tumor:blood and tumor:brain ratios; (*iii*) no residual brain tumors in rats that survived for 180 days after BNCT-regimen with PBC_2 administered via CED; (*iv*) 70% of animal survival at 180 days after BNCT-regimen when it was combined with BPA.[179]

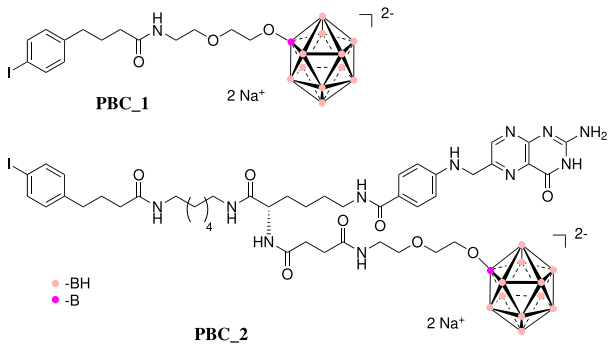

Figure 27. PBC containing potential BNCT agents able to interact with albumin via the 4-iodophenylbutanoyl-moiety.

Another strategy used to incorporate PBC into potential BNCT agents has been the association to structural fragments with the ability to recognize specific biomolecules differentially expressed under pathological conditions such as cancers. In this sense, one of the current strategies has been to improve boron delivery to cancer cells using boron-containing-molecules that recognize the glucose transporter GLUT1 overexpresses in head and neck cancers.[180] Thus, the *o*-carboranyl-glucose derivatives PBC_3 and PBC_4 (Figure 28), synthesized by coupling reaction between and alkyne-glucose derivative with the decaborane complex $B_{10}H_{12}(MeCN)_2$, displayed better boron CAL 27-cell uptake than BPA or BSH and lower or similar toxicity than BSH. Later, the same research group reported new glucose derivatives but, in this case, *ortho*- and *meta*-carboranyls prepared via nucleophilic substitutions between 6-iodomethylglucose and the corresponding mercapto-carborane. In this case, the *m*-carboranyl-derivatives PBC_5 and PBC_6 (Figure 28) displayed better biological behaviors, in the boron uptake and in the cytotoxicity, than both BSH and the corresponding *o*-carboranyl-analogues but lower boron uptake and higher cytotoxicity than the previous developed derivatives, i.e., PBC_3 and PBC_4. Additionally, high GLUT1 affinity were displayed by some of them and, in some cases, higher than natural substrate D-glucose, e.g., PBC_4 (IC_{50} = 32.07 μM) > PBC_3 (IC_{50} = 43.96 μM) > PBC_5 (IC_{50} = 120.6 μM) > D-glucose (IC_{50} > 1000 μM) > PBC_6 (IC_{50} = 2128 μM). Unfortunately, the authors have not described, to date, BNCT *in vitro* or *in vivo* studies.

The tyrosine kinases receptors (TKR), that are involved in cells-communication, -proliferation, -differentiation, -survival, and -migration, have also been taken into account to design agents, useful for BNCT, able to interact with them and also carrying PBC. Since 2017, we have been working on this type of hybrid agents taking some structural components of TKR inhibition pharmacophores, i.e., the 4-anilinoquinazoline framework found in erlotinib and lapatinib and the indolin-2-one fragment found in sunitinib, and different PBC, i.e., *closo*-dodecaborate-, cobaltabis(1,2-dicarbollide)-, *o*- and *m*-carborane-fragment, and connectors, i.e., 1,2,3-triazolalkyl- and benzylalkynyl-moieties (PBC_7-PBC_12, Figure 29).[181-183] Thus, compared to the corresponding parent compound, compounds PBC_7, PBC_9, and PBC_11 exhibited stronger cytotoxic activity against various cell types, including U87 MG, C6 and F98 glioma cells, and HT-29 colorectal adenocarcinoma cells. This biological characteristic is noteworthy when considering hybrid agents but is not always relevant in BNCT. Due to their bioactivities, all of the dodecaborate- and benzylalkynyl-derivatives, such as compounds PBC_8 and PBC_12, respectively, were not structurally interesting. Furthermore, a few of them demonstrated intriguing TKR-inhibition properties. For instance, compound PBC_7 was ten times more potent against wild type epidermal growth factor receptor (EGFR) than erlotinib, the parent compound,[184] while compound PBC_11 demonstrated inhibition of FLT3, PDGFR-α and β, KIT, CSF1R, and VEGFR2, but not as much of AMP-activated protein kinase and ribosomal S6 kinase RSK1, which made sunitinib cardiotoxic.[185] The most relevant aspect in the studies, was the excellent *in vitro* BNCT performances for PBC_7, PBC_9, PBC_10 and PBC_11 showing, in general, selective and better boron

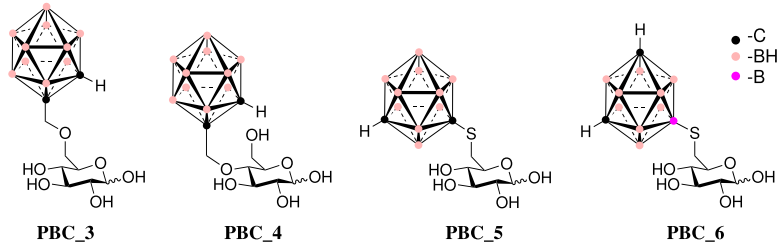

Figure 28. Some PBC derivatives with ability to recognize GLUT1 differentially expressed under pathological conditions such as cancers.

accumulation in studied cells and lower cell-survival after neutron irradiation than BPA, in the same doses and conditions.[182,183,186] On the other hand, according to Raman confocal microscopy (Figure 30), PBC_7 retains erlotinib cellular-uptake mechanism observing boron at the membrane level, which could indicate the interaction with EGFR, and also at the intracellular level, which could not rule out endocytosis process. Furthermore, compounds PBC_7 and PBC_11, which have drug-like properties, turned out to be excellent antitumoral agents in a murine model of U87 MG glioblastoma.[185-188]

Recently,[189] using "three-in-one" strategy erlotinib-pharmacophore containing PBC were developed (e.g., PBC_13, Figure 29) with promising *in vivo* results. The compounds were designed by incorporating boron content units, 1,3,2-dioxaborolan-2-yl or *o*-carboranyl moieties, a 4-anilinoquinazolinyl-framework EGFR-targeting unit and a donor-acceptor type aggregation-induced emission imaging unit, 1,8-naphthalimidyl group as a strong acceptor. They demonstrated excellent properties for imaging purposes, highly selective accumulations in tumors, and *in vivo* tumor growth suppression after neutron irradiation and ^{10}B-PBC_13 dosage.

The microenvironment and heterogeneity of solid tumors, specifically hypoxia which is involved in therapy resistance, disease progression, immune system evasion and metastasis, have been used considered in the PBC containing agents' research for BNCT. For that, the tumoral-hypoxic nitroimidazole pharmacophore, that after undergo bioreductive activation the amine-metabolite is confined in the acidic hypoxic-tumoral tissues, was combined to *o*-carboranyl moiety and additionally a fragment, i.e., aminoacidic derivative, able to targeting LAT1.[190] The *in vitro* uptake of boron from compound PBC_14

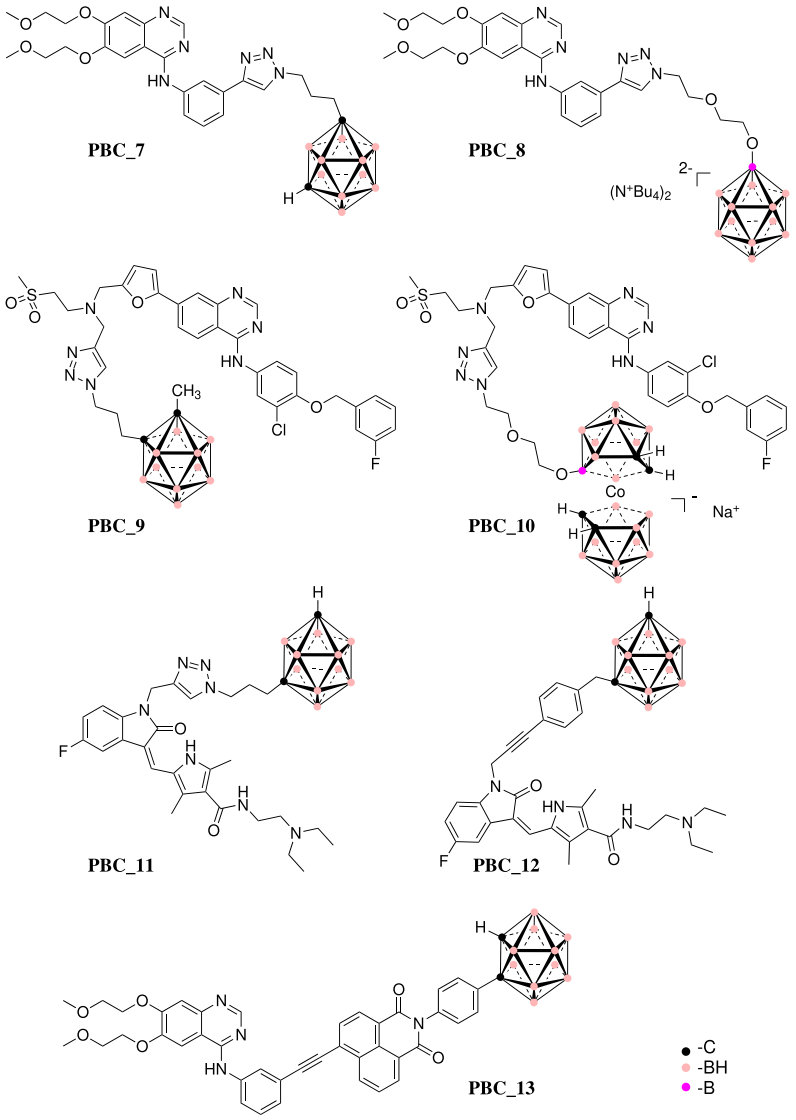

Figure 29. Some PBC derivatives with potential ability to recognize TKR differentially expressed under pathological conditions such as cancers.

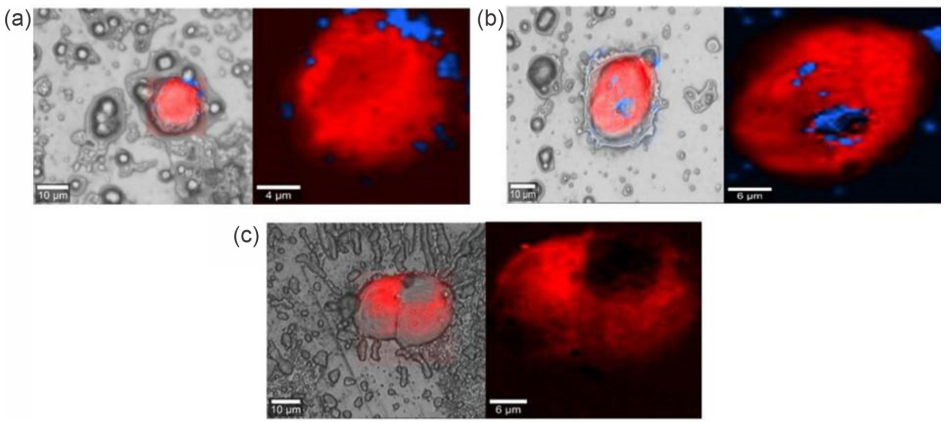

Figure 30. White-light optical image merge Raman image (left) and Raman image (right) of U87 MG incubated with PBC_7 for 12 h (a) or 24 h (b). (c) Control untreated cells (adapted from reference 186).

(Figure 31) into hypoxic tumoral regions was 70 times higher than the corresponding from BPA while *in vivo* studies indicated a prolonged periods of tumoral boron-trapped, in therapeutic concentration, and tumor:blood ratios higher than 3 after 4 h post-injection. Although PBC_14 has not shown significant *in vivo* toxicity, the authors have not yet studied it in BNCT protocols.

COX-2 is highly expressed in the head and neck cancers consequently it has been chosen to target boron containing compounds to cancerous tissues.[191] The hybrid celecoxib-*o*-carboranyl PBC_15 (Figure 31) displayed high COX-2 selectivity and higher *in vitro* tongue squamous cell carcinoma CAL 27 cells selectivity and uptake than BSH. During BNCT, PBC_15 affected the cytoskeleton and induced the cellular apoptosis by breaking DNA double strands, generating excess reactive oxygen species and down-regulating the expression of some cytokines.

The expression of FRα in a variety of tumors has been employed to design hybrids folate-PBC derivatives for BNCT. In this sense, Gruzdev *et al.*[192] have described bis-amides derived from folic acid attaching *closo*- or *nido*-carboranes (such as PBC_16 and PBC_17, Figure 31) via alkylcarbamoyl connector. These compounds were soluble in alkaline aqueous solution, displayed low cytotoxicity in the studied cells, among them U87 MG, and accumulated boron in *in vitro* experiments with U87 MG at least, for PBC_17, 7 times more than BSH, BPA and other folic acid-derivatives. Unfortunately, the authors have not described, to date, BNCT *in vitro* or *in vivo* studies.

Another employed target to develop agents for BNCT was the matrix metalloproteinases (MMP) overexpressed at the surface of the tumor cell. Hydroxamate, with capability to be ligands for MMP, bearing *o*-carboranes were prepared via [3 + 2] click chemistry between an alkyne-hydroxamate derivative and an *o*-carboranylpropylazide, due to the direct alkyne-decaborane complex $B_{10}H_{12}(MeCN)_2$ insertion was unsuccessful.[193] They have excellent potencies against MMP-2, -9 and -13 and *in vitro* BNCT effects. For example, hydroxamate-carborane PBC_18 (Figure 31) displayed a BNCT effect three times higher than BPA in squamous cell carcinoma (SCC)VII and effectively killed glioma U87 delta EGFR cells.

An additional alternative to generate hybrid agents to be used in BNCT has been employed substructures with ability to intercalate to DNA for example the acridine heterocycle. In this regard, the hybrid benzo[*b*]acridone-*o*-carborane PCB_19[194] (Figure 31) displayed: (*i*) minimal toxicity against U87 MG cells at concentration up to 200 µM, for the authors a promising property as potential BNCT agent; (*ii*) significant accumulation in the cells, near to 3×10^{10} ^{10}B atoms *per* cell, located mainly in the cytoskeleton; (*iii*) double strand breaks and late damage upon *in vitro* BNCT simulation. On the other hand, from an azidoacridine reacting via copper(I)-catalyzed 1,3-dipolar [3 + 2] cycloaddition process the cobalt bis(dicarbollide) fragment was incorporated generating compounds such as PBC_20 (Figure 31) as another DNA intercalating agent.[188] It displayed antiproliferative activity against some tumoral and non-tumoral cells and some level of interaction with DNA. Unfortunately, the authors have not described, to date, BNCT *in vitro* or *in vivo* studies.

Lastly, alternative methods have recently been employed to incorporate PBC into entities that may have use in BNCT. These methods include those reported by Kaniowski *et al.*[195] in the development of biopharmaceuticals derived from oligonucleotides coupled to FESAN or those described by Shirakawa *et al.*[195] or Kawasaki *et al.*[195] in the development of drug-delivery systems that facilitate the boron accumulation and retention in tumor tissues by enhanced permeation and retention (EPR) effect.[195]

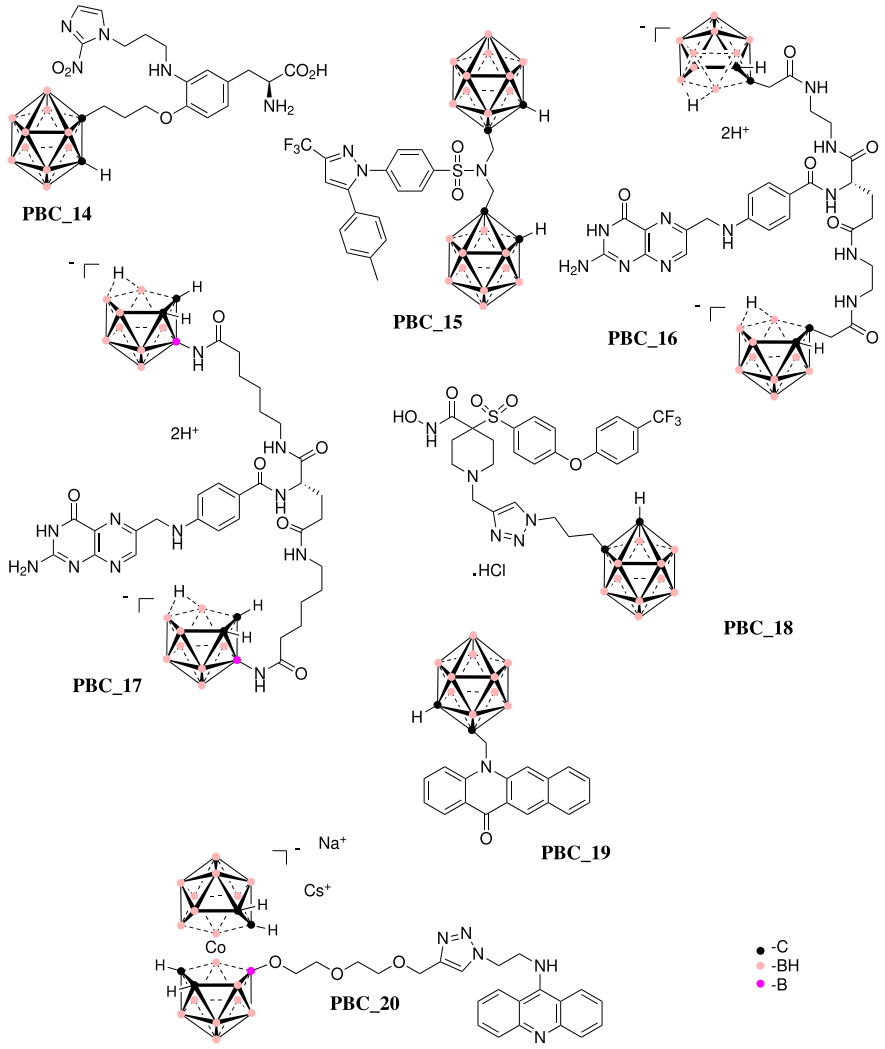

Figure 31. Other PBC derivatives with potential ability to recognize specific biomolecules differentially expressed under pathological conditions such as cancers.

3.3. Benefits of PBC as building block in BNCT agent design; "drug-like" properties of PBC-containing compounds

The main benefit of PBC as building block in BNCT agent design is the large contribution of boron atoms *per* agent molecule. In addition, other PBC properties could be useful considering the contribution of the BNCT agent, for example: (*i*) their B–H low polarity that contribute to a molecular polarity appropriate for membrane passive transport; (*ii*) their wide range of potential noncovalent interactions with biosystems, such as hydrogen bonds, dihydrogen bonds and bridging interactions;[184] (*iii*) their inherent capacity to spontaneously generate micrometer- to nano-sized particles in aqueous solutions, which could be used in EPR effect.[196] Another relevant properties of PBC in the BNCT agent design processes are: (*i*) the bioisosteric replacement cyclic hydrocarbon, such as adamantane and benzene, to carborane; (*ii*) the three dimensional and orthogonal functionalization better than in 2D-benzene.

Given that PBC are relatively new moiety in the field of medicinal chemistry, comparing to traditional organic-frameworks, there are still many questions regarding their contributions to the drug-like properties of a new agent, among others, metabolic stability, toxicity, excretion pathways.

One of the most studied properties has been the lipophilicity of PBC containing compounds determining the partition coefficient, for neutral derivatives, or the distribution coefficient, for the ionic ones.[181,183,197-199] Different determination of lipophilicity descriptors, such as Hansch-Fujita hydrophobic parameter π, were done being the studies of Endo and co-workers[200,201] the most comprehensive (Table 7). The presence of hydride-like hydrogens at the boron atoms makes the carboranyl-substituent more hydrophobic than *t*-butyl- or phenyl-substituent. When there is only one CH in the cluster, the

substituent is more hydrophobic than the adamantyl group while when there are two CHs in the cluster the substituent is more hydrophilic than adamantyl. This could be due to the acidity of the CH group (see section 2.3.1).

Table 7. Fragmentary lipophilic descriptor for carboranyl substituent

Substituent	π	Reference
p-Carboran-1-yl	+4.44	200
o-Carboran-1-yl	+4.30	200
m-Carboran-1-yl	+4.26	200
m-Carboran-2-yl	+4.08	200
1-Adamantyl	+4.04	200
p-Carboran-2-yl	+4.01	200
o-Carboran-3-yl	+3.71	200
m-Carboran-9-yl	+3.17	200
Cyclohexyl	+2.97	200
o-Carboran-9-yl	+2.69	200
t-Butyl	+1.79	197
Phenyl	+1.69	197

The interaction with serum albumin, the most abundant protein in mammalian blood, was studied in selected PBC containing compounds.[202] The metallacarboranes, COSAN and FESAN, have the strongest interaction with albumin among the tested clusters being the PBC interactions strength: metallacarboranes $[M(C_2B_9H_{11})_2]^-$ > *p*-carboranes ($C_2B_{10}H_{12}$) >> dodecaborate anion $[B_{12}H_{12}]^{2-}$. According to the different performed studies metallacarboranes first specifically interact with the binding cavity of albumin and then, as compound concentrations increase, interact non-specifically with the protein surface.

Assuming that the inorganic abiotic nature of PBC slows down the enzymatic degradation of the potential BNCT agent, it is expected to lead to greater metabolic stability and therefore minimal presence of toxic metabolites. However, metabolism and toxicity studies of PBC-containing potential drugs are still very rare in the literature and they should be systematically carried out. Some studies related to *in vitro* metabolism of PBC_7 (Figure 29),[184] physiological environment stability of PBC_7 and PBC_13 (Figure 29),[184,189] and mutagenicity and *in vivo* toxicity of PBC_7 and PBC_11 (Figure 29)[185,187] have been performed finding adequate drug-like properties for these compounds.

4. Conclusions and Future Outlook

Through this review, it has been possible to analyze the relevant reactivity of boranes, metallacarboranes, and carboranes. Specifically, the carborane scaffold has the possibilities of regioselective derivatization at each vertex (–CH and –BH) which could be spectroscopically characterized properly. Simultaneously, according to the current landscape of boron neutron capture therapy the polyhedral boron clusters shed light on fundamental achievements, advances and challenges related to their application in this pharmacological tool. Further, the polyhedral boron clusters have been exploited in drug design, examining their application not only in BNCT but also as standalone chemotherapeutic agents.

This dual functionality underscores the versatility of high-boron-content compounds in the realm of medicinal chemistry, offering promising avenues for the development of novel therapeutic strategies. Furthermore, they have drug-like properties, although these must be more thoroughly verified. Looking ahead, there are many promising opportunities for improving and optimizing boron neutron capture therapy by polyhedral boron clusters.

Future research endeavors should focus on fine-tuning the design and synthesis of boron-rich compounds, with an emphasis on enhancing their selectivity, bioavailability, and therapeutic efficacy. Additionally, exploring novel delivery strategies and combining BNCT with other therapeutic modalities could open new avenues for synergistic cancer treatments. Advances in nanotechnology, targeted drug delivery systems, and imaging techniques are anticipated to contribute to the continued progress of BNCT, making it more accessible and effective in clinical settings.

Collaborative efforts between researchers, clinicians, and industry stakeholders will be pivotal in translating these advancements from bench to bedside. As we move forward, the potential integration of polyhedral boron clusters into broader medicinal chemistry applications should not be overlooked, offering opportunities for innovation in drug discovery and development beyond the realm of cancer therapy.

Marcos Couto *obtained his PhD degree in Chemistry in 2019 at the Facultad de Química, Universidad de la República, Uruguay, under the supervision of Prof Clara Viñas and Hugo Cerecetto. He successfully completed an MBA in 2021 and subsequently undertook a postdoctoral research period at ICMAB-CSIC, Spain, in 2022. He has authored 17 scientific articles in international peer-reviewed journals and contributed to a book chapter, predominantly serving as corresponding author or first author. Since 2023, Dr Couto*

has assumed leadership of the Medicinal Organic Chemistry Group at the Facultad de Ciencias, Instituto de Química Biológica, Universidad de la República, Uruguay.

Hugo Cerecetto *completed his PhD in Medicinal Chemistry in 1994 under the supervision of Dr Antonio Monge at the Universidad de Navarra (Spain). Between 1987 and 2012 he was Organic Chemistry professor at the Facultad de Química-Universidad de la República (Uruguay) and in 2013 he joined at the Area of Radiofarmacia, at the Centro de Investigaciones Nucleares-Universidad de la República (Uruguay), as responsible. Almost 310 papers in the field of Medicinal Chemistry and specialized R+D+i of new drugs have been published by him. For his publications, he received the national 2010 Elsevier-SCOPUS Prize.*

References

1. Locher, G. L.; *AJR, Am. J. Roentgenol.* **1936**, *36*, 1.
2. Kruger, P. G.; *Proc. Natl. Acad. Sci. U. S. A.* **1940**, *26*, 181. [Crossref]
3. Deagostino, A.; Protti, N.; Alberti, D.; Boggio, P.; Bortolussi, S.; Altieri, S.; Geninatti Crich, S.; *Future Med. Chem.* **2016**, *8*, 899. [Crossref]
4. Barth, R. F.; Soloway, A. H.; Brugger, R. M.; *Cancer Invest.* **1996**, *14*, 534. [Crossref]
5. Cerecetto, H.; Couto, M. In *Glioma - Contemporary Diagnostic and Therapeutic Approaches*; Omerhodzic, I.; Arnautovic, K., eds.; IntechOpen Limited: UK, 2019. [Crossref]
6. Yanagie, H.; Higashi, S.; Seguschi, K.; Ikushima, I.; Fujihara, M.; Nonaka, Y.; Oyama, K.; Maruyama, S.; Hatae, R.; Suzuki, M.; Masunaga, S. I.; Kinashi, T.; Sakurai, Y.; Tanaka, H.; Kondo, N.; Narabayashi, M.; Kajiyama, T.; Maruhashi, A.; Ono, K.; Nakajima, J.; Ono, M.; Takahashi, H.; Eriguchi, M.; *Appl. Radiat. Isot.* **2014**, *88*, 32. [Crossref]
7. Hiratsuka, J.; Kamitani, N.; Tanaka, R.; Yoden, E.; Tokiya, R.; Suzuki, M.; Barth, R. F.; Ono, K.; *Cancer Commun.* **2018**, *38*, 38. [Crossref]
8. Miyatake, S. I.; Wanibuchi, M.; Hu, N.; Ono, K.; *J. Neurooncol.* **2020**, *149*, 1. [Crossref]
9. Fukuda, H.; *Cells* **2021**, *10*, 2881. [Crossref]
10. Wang, L. W.; Liu, Y. W. H.; Chu, P. Y.; Liu, H. M.; Peir, J. J.; Lin, K. H.; Huang, W. S.; Lo, W. L.; Lee, J. C.; Lin, T. Y.; Liu, Y. M.; Yen, S. H.; *Cancers* **2023**, *15*, 2762. [Crossref]
11. Marforio, T. D.; Carboni, A.; Calvaresi, M.; *Cancers* **2023**, *15*, 4944. [Crossref]
12. Hirose, K.; Konno, A.; Hiratsuka, J.; Yoshimoto, S.; Kato, T.; Ono, K.; Otsuki, N.; Hatazawa, J.; Tanaka, H.; Takayama, K.; Wada, H.; Suzuki, M.; Sato, M.; Yamaguchi, H.; Seto, I.; Ueki, Y.; Iketani, S.; Imai, S.; Nakamura, T.; Ono, T.; Endo, H.; Azami, Y.; Kikuchi, Y.; Murakami, M.; Takai, Y.; *Radiother. Oncol.* **2021**, *155*, 182 [Crossref]; Matsumura, A.; Asano, T.; Hirose, K.; Igaki, H.; Kawabata, S.; Kumada, H.; *Cancer Biother. Radiopharm.* **2023**, *38*, 201. [Crossref]
13. Skwierawska, D.; López-Valverde, J. A.; Balcerzyk, M.; Leal, A.; *Cancers* **2022**, *14*, 2865. [Crossref]
14. Grams, R. I.; Santos, W. L.; Scorei, I. R.; Abad-García, A.; Rosenblum, C.; Bita, A.; Cerecetto, H.; Viñas, C.; Soriano-Ursúa, M. A.; *Chem. Rev.* **2024**, *124*, 2441. [Crossref]
15. Sweet, W. H.; *N. Engl. J. Med.* **1951**, *245*, 875. [Crossref]
16. Farr, L. E.; Robertson, J. S.; Stickley, E. E.; Bagnall, H. J.; Easterday,O.D.; Kahle, W. In *Proceedings on the Second United Nations International Conference on the Peaceful Uses of Atomic Energy*; United Nations: Geneva, 1958. [Link]
17. Sweet, W. H.; Soloway, A. H.; Brownell, G. L.; *Acta Radiol.: Ther., Phys., Biol.* **1963**, *1*, 114. [Crossref]
18. Lamba, M.; Goswami, A.; Bandyopadhyay, A.; *Chem. Commun.* **2021**, *57*, 827. [Crossref]
19. Zaidlewicz, M.; Sokół, W.; Wolan, A.; Cytarska, J.; Tafelska-Kaczmarek, A.; Dzielendziak, A.; Prewysz-Kwinto, A.; *Pure Appl. Chem.* **2003**, *75*, 1349. [Crossref]
20. Nakamura, H.; Fujiwara, M.; Yamamoto, Y.; *Bull. Chem. Soc. Jpn.* **2001**, *73*, 231. [Crossref]
21. Nakamura, H.; Fujiwara, M.; Yamamoto, Y.; *J. Org. Chem.* **1998**, *63*, 7529. [Crossref]
22. Snyder, H. R.; Reedy, A. J.; Lennarz, W. J.; *J. Am. Chem. Soc.* **1958**, *80*, 835. [Crossref]
23. Fukuda, H.; Hiratsuka, J.; *Appl. Radiat. Isot.* **2020**, *166*, 109308. [Crossref]
24. Balcer, E.; Giebułtowicz, J.; Sochacka, M.; Ruszczyńska, A.; Muszyńska, M.; Bulska, E.; *Molecules* **2023**, *28*, 6552. [Crossref]
25. Nomoto, T.; Inoue, Y.; Yao, Y.; Suzuki, M.; Kanamori, K.; Takemoto, H.; Matsui, M.; Tomoda, K.; Nishiyama, N.; *Sci. Adv.* **2020**, *6*, eaaz1722. [Crossref]
26. Nomoto, T.; Yao, Y.; Inoue, Y.; Suzuki, M.; Kanamori, K.; Takemoto, H.; Matsui, M.; Tomoda, K.; Nishiyama, N.; *J. Controlled Release* **2021**, *332*, 184. [Crossref]
27. Meunier, B.; *Acc. Chem. Res.* **2008**, *41*, 69. [Crossref]
28. Rondina, A.; Fossa, P.; Orro, A.; Milanesi, L.; De Palma, A.; Perico, D.; Mauri, P.L.; D'Ursi, P.; *Cells* **2021**, *10*, 3225. [Crossref]
29. Itoh, T.; Tamura, K.; Ueda, H.; Tanaka, T.; Sato, K.; Kuroda, R.; Aoki, S.; *Bioorg. Med. Chem.* **2018**, *26*, 5922 [Crossref]; Campkin, D. M.; Shimadate, Y.; Bartholomew, B.; Bernhardt, P. V.; Nash, R. J.; Sakoff, J. A.; Kato, A.; Simone, M. I.; *Molecules* **2022**, *27*, 3447 [Crossref]; Confalonieri, L.; Imperio, D.; Erhard, A.; Fallarini, S.; Compostella, F.; Del Grosso, E.; Balcerzyk, M.; Panza, L.; *ACS Omega* **2022**, *7*, 48340. [Crossref]; Simone, M. I.; *Molecules* **2023**, *28*, 4321. [Crossref]

30. Xiang, J.; Ma, L.; Gu, Z.; Jin, H.; Zhai, H.; Tong, J.; Liang, T.; Li, J.; Ren, Q.; Liu, Q.; *Cells* **2022**, *11*, 1173. [Crossref]
31. Takahashi, K.; Nakamura, H.; Furumoto, S.; Yamamoto, K.; Fukuda, H.; Matsumura, A.; Yamamoto, Y.; *Bioorg. Med. Chem.* **2005**, *13*, 735. [Crossref]
32. Soloway, A. H.; Hatanaka, H.; Davis, M. A.; *J. Med. Chem.* **1967**, *10*, 714 [Crossref]; Hatanaka, H.; Sweet, W. H.; Sano, K.; Ellis, F.; *Pure Appl. Chem.* **1991**, *63*, 373. [Crossref]
33. Kageji, T.; Nakagawa, Y.; Kitamura, K.; Matsumoto, K.; Hatanaka, H.; *J. NeuroOncol.* **1997**, *33*, 117. [Crossref]
34. Hideghéty, K.; Sauerwein, W.; Wittig, A.; Götz, C.; Paquis, P.; Grochulla, F.; Haselsberger, K.; Wolbers, J.; Moss, R.; Huiskamp, R.; Fankhauser, H.; de Vries, M.; Gabel, D.; *J. Neuro-Oncol.* **2003**, *62*, 145. [Crossref]
35. Elhanati, G.; Salomon, Y.; Bendel, P.; *Cancer Lett.* **2001**, *172*, 127. [Crossref]
36. Mi, P.; Yanagie, H.; Dewi, N.; Yen, H. C.; Liu, X.; Suzuki, M.; Sakurai, Y.; Ono, K.; Takahashi, H.; Cabral, H.; Kataoka, K.; Nishiyama, N.; *J. Controlled Release* **2017**, *254*, 1. [Crossref]
37. Futamura, G.; Kawabata, S.; Nonoguchi, N.; Hiramatsu, R.; Toho, T.; Tanaka, H.; Masunaga, S. I.; Hattori, Y.; Kirihata, M.; Ono, K.; Kuroiwa, T.; Miyatake, S. I.; *Rad. Oncol.* **2017**, *12*, 26. [Crossref]
38. Takeuchi, K.; Hattori, Y.; Kawabata, S.; Futamura, G.; Hiramatsu, R.; Wanibuchi, M.; Tanaka, H.; Masunaga, S. I.; Ono, K.; Miyatake, S. I.; Kirihata, M.; *Cells* **2020**, *9*, 1551. [Crossref]
39. Grimes, R. N.; *Carboranes*; Academic Press: UK, 2016.
40. Price, W. C.; *J. Chem. Phys.* **1947**, *15*, 614. [Crossref]
41. Stock, A.; Massenez, C.; *Chem. Ber.* **1912**, *45*, 3539. [Crossref]
42. Stock, A.; *Hydrides of Boron and Silicon*; Cornell University Press: Ithaca, New York, 1933.
43. Eberhardt, W. H.; Crawford, B.; Lipscomb, W. N.; *J. Chem. Phys.* **1954**, *22*, 989. [Crossref]
44. Hoffmann, R.; Lipscomb, W. N.; *J. Chem. Phys.* **1962**, *37*, 2872. [Crossref]
45. Klein, M. J.; Harrison, B. C.; Solomon, I. J.; *J. Am. Chem. Soc.* **1958**, *80*, 4149. [Crossref]
46. Faust, J. P. In *Borax to Boranes: A Collection of Papers*; Gould, R. F., ed.; American Chemical Society: Washington DC, USA, 1961. [Crossref]
47. Bykov, A. Y.; Razgonyaeva, G. A.; Maltseva, N. N.; Zhizhin, K. Y.; Kuznetsov, N. T.; *Russ. J. Inorg. Chem.* **2012**, *57*, 471. [Crossref]
48. Sauer, J. C.; *US 3457050 A*, **1969**.
49. Judd, G. F.; *US 2968534 A*, **1961**.
50. Miller, H. C.; Miller, N. E.; Muetterties, E. L.; *J. Am. Chem. Soc.* **1963**, *85*, 3885. [Crossref]
51. Chong, M.; Matsuo, M.; Orimo, S. I.; Autrey, T.; Jensen, C. M.; *Inorg. Chem.* **2015**, *54*, 4120. [Crossref]
52. Sivaev, I. B.; Bregadze, V. I.; Sjoberg, S.; *Collect. Czech. Chem. Commun.* **2002**, *67*, 679. [Crossref]
53. Wade, K.; *J. Chem. Soc. D* **1971**, 792. [Crossref]
54. Wade, K. In *Advances in Inorganic Chemistry and Radiochemistry*; Emeléus, H. J.; Sharpe, A. G., eds.; Academic Press: San Francisco, USA, 1976.
55. Mingos, D. M. P.; Wales, D. J.; *Introduction to Cluster Chemistry*; Prentice Hall: Englewood Cliffs, USA, 1990.
56. Welch, A. J.; *Chem. Commun.* **2013**, *49*, 3615. [Crossref]
57. Longuet-Higgins, H. C.; Roberts, M. V.; *Proc. Roy. Soc.* **1955**, *A230*, 110. [Crossref]
58. Hawthorne, M. F.; Pitochelli, A. R.; *J. Am. Chem. Soc.* **1960**, *82*, 3328 [Crossref]; Hawthorne, M. F.; Pitochelli, A. R.; *J. Am. Chem. Soc.* **1959**, *81*, 5519. [Crossref]
59. Fox, M. A.; Wade, K.; *Pure Appl. Chem.* **2003**, *75*, 1315. [Crossref]
60. Rudolph, R. W.; *Acc. Chem. Res.* **1976**, *9*, 446. [Crossref]
61. Hosmane, N. S.; *Boron Science: New Technologies and Applications*; Taylor & Francis Books/CRC: Boca Raton, US, 2011. [Crossref]
62. Poater, J.; Solà, M.; Viñas, C.; Teixidor, F.; *Angew. Chem., Int. Ed.* **2014**, *53*, 12191. [Crossref]
63. Schleyer, P. R.; Najafian, K.; *Inorg. Chem.* **1998**, *37*, 3454. [Crossref]
64. El-Zaria, M. E.; Keskar, K.; Genady, A. R.; Ioppolo, J. A.; McNulty, J.; Valliant, J. F.; *Angew. Chem.* **2014**, *126*, 5256. [Crossref]
65. Plešek, J.; Plzák, Z.; Stuchlík, J.; Heřmánek, S.; *Collect. Czech. Chem. Commun.* **1981**, *46*, 1748 [Crossref]; Jelínek, T.; Plešek, J.; Mareš, F.; Heřmánek, S.; Štíbr, B.; *Polyhedron* **1987**, *6*, 1981. [Crossref]
66. For selected examples, see: Potenza, J. A.; Lipscomb, W. N.; Vickers, G. D.; Schroeder, H.; *J. Am. Chem. Soc.* **1966**, *88*, 628 [Crossref]; Andrews, J. S.; Zayas, J.; Jones, M.; *Inorg. Chem.* **1985**, *24*, 3715 [Crossref]; Zheng, Z.; Jiang, W.; Zinn, A. A.; Knobler, C. B.; Hawthorne, M. F.; *Inorg. Chem.* **1995**, *34*, 2095 [Crossref]; Zheng, Z.; Knobler, C. B.; Mortimer, M. D.; Kong, G.; Hawthorne, M. F.; *Inorg. Chem.* **1996**, *35*, 1235 [Crossref]; Herzog, A.; Maderna, A.; Harakas, G. N.; Knobler, C. B.; Hawthorne, M. F.; *Chem. Eur. J.* **1999**, *5*, 1212 [Crossref]; Teixidor, F.; Barberà, G.; Vaca, A.; Kivekäs, R.; Sillanpää, R.; Oliva, J.; Viñas, C.; *J. Am. Chem. Soc.* **2005**, *127*, 10158 [Crossref]; Teixidor, F.; Barberà, G.; Viñas, C.; Sillanpää, R.; Kivekäs, R.; *Inorg. Chem.* **2006**, *45*, 3496 [Crossref]; Spokoyny, A. M.; Machan, C. W.; Clingerman, D. J.; Rosen, M. S.; Wiester, M. J.; Kennedy, R. D.; Stern, C. L.; Sarjeant, A. A.; Mirkin, C. A.; *Nat. Chem.* **2011**, *3*, 590. [Crossref]
67. Wiesboeck, R. A.; Hawthorne, M. F.; *J. Am. Chem. Soc.* **1964**, *86*, 1642 [Crossref]; Hawthorne, M. F.; Young, D. C.; Garrett, P. M.; Owen, D. A.; Schwerin, S. G.; Tebbe, F. N.; Wegner, P. A.; *J. Am. Chem. Soc.* **1968**, *90*, 862. [Crossref]
68. Zakharkin, L. I.; Kalinin, V. N.; *Tetrahedron Lett.* **1965**, *6*, 407. [Crossref]

69. Tomita, H.; Luu, H.; Onak, T.; *Inorg. Chem.* **1991**, *30*, 812. [Crossref]
70. Fox, M. A.; Gill, W. R.; Herbertson, P. L.; MacBride, J. A. H.; Wade, K.; Colquhoun, H. M.; *Polyhedron* **1996**, *15*, 565. [Crossref]
71. Getman, T. D.; *Inorg. Chem.* **1998**, *37*, 3422. [Crossref]
72. Yoo, J.; Hwang, J. W.; Do, Y.; *Inorg. Chem.* **2001**, *40*, 568. [Crossref]
73. Davidson, M. G.; Fox, M. A.; Hibbert, T. G.; Howard, J. A. K.; Mackinnon, A.; Neretin, I. S.; Wade, K.; *Chem. Commun.* **1999**, 1649. [Crossref]
74. Batsanov, A. S.; Copley, R. C. B.; Davidson, M. G.; Fox, M. A.; Hibbert, T. G.; Howard, J. A. K.; Wade, K.; *J. Cluster Sci.* **2006**, *17*, 119. [Crossref]
75. Zakharkin, L. I.; Kirillova, V. S.; *Russ. Chem. Bull.* **1975**, *24*, 2484. [Crossref]
76. Hawthorne, M. F.; Young, D. C.; Wegner, P. A.; *J. Am. Chem. Soc.* **1965**, *87*, 1818. [Crossref]
77. Bennour, I.; Cioran, A.; Teixidor, F.; Viñas, C.; *Green Chem.* **2019**, *21*, 1925. [Crossref]
78. Churchill, M. R.; Gold, K.; Francis, J. N.; Hawthorne, M. F.; *J. Am. Chem. Soc.* **1969**, *91*, 1222. [Crossref]
79. Plešek, J.; Heřmánek, S.; *Czech. Chem. Commun.* **1995**, *60*, 1297 [Crossref]; Franken, A.; Plešek, J.; Nachtigal, C.; *Collect. Czech. Chem. Commun.* **1997**, *62*, 746. [Crossref]
80. Llop, J.; Masalles, C.; Viñas, C.; Teixidor, F.; Sillanpää, R.; Kivekäs, R.; *Dalton Trans.* **2003**, *4*, 556. [Crossref]
81. Sivaev, I.; Starikova, Z.; Sjöberg, S.; Bregadze, V. I.; *J. Organomet. Chem.* **2002**, *649*, 1. [Crossref]
82. Plešek, J.; Grüner, B.; Heřmánek, S.; Báča, J.; Mareček, V.; Jänchenová, J.; Lhotský, A.; Holub, K.; Selucký, P.; Rais, J.; Císařová, I.; Čáslavský, J.; *Polyhedron* **2002**, *21*, 975. [Crossref]
83. Viñas, C.; Bertran, J.; Gomez, S.; Teixidor, F.; Dozol, J. F.; Rouquette, H.; Kivekäs, R.; Sillanpää, R.; *Dalton Trans.* **1998**, *17*, 2849. [Crossref]
84. Grüner, B.; Mikulášek, L.; Báča, J.; Císařová, I.; Böhmer, V.; Danila, C.; Reinoso-García, M.; Verboom, W.; Reinhoudt, D.; Casnati, A.; Ungaro, R.; *Eur. J. Org. Chem.* **2005**, 2022. [Crossref]
85. Olejniczak, A. B.; Plešek, J.; Lesnikowski, Z. J.; *Chem. Eur. J.* **2006**, *13*, 311. [Crossref]
86. Matejicek, P.; Cígler, P.; Olejniczak, A. B.; Andrysiak, A.; Wojtczak, B.; Prochazka, K.; Lesnikowski, Z. J.; *Langmuir* **2008**, *24*, 2625. [Crossref]
87. Farràs, P.; Teixidor, F.; Kivekäs, R.; Sillanpää, R.; Viñas, C.; Grüner, B.; Cisarova, I.; *Inorg. Chem.* **2008**, *47*, 9497. [Crossref]
88. Juarez-Perez, E. J.; Núñez, R.; Viñas, C.; Sillanpää, R.; Teixidor, F.; *Eur. J. Inorg. Chem.* **2010**, *2010*, 2385. [Crossref]
89. Hermansson, K.; Wójcik, M.; Sjöberg, S.; *Inorg. Chem.* **1999**, *38*, 6039. [Crossref]
90. Zakharkin, L. I.; Ogorodnikova, N. A.; *J. Organomet. Chem.* **1968**, *12*, 13. [Crossref]
91. Douglass, A. G.; Pakhomov, S.; Reeves, B.; Janousek, Z.; Kaszynski, P.; *J. Org. Chem.* **2000**, *65*, 1434. [Crossref]
92. Heying, T. L.; Ager, J. W.; Clark, S. L.; Alexander, R. P.; Papetti, S.; Reid, J. A.; Trotz, S. I.; *Inorg. Chem.* **1963**, *2*, 1097. [Crossref]
93. L'Esperance, R. P.; Li, Z. H.; Van Engen, D.; Jones, M.; *Inorg. Chem.* **1989**, *28*, 1823. [Crossref]
94. Thomas, J.; Hawthorne, M. F.; *Chem. Commun.* **2001**, *18*, 1884 [Crossref]; Jiang, W.; Chizhevsky, I. T.; Mortimer, M. D.; Chen, W.; Knobler, C. B.; Johnson, S. E.; Gomez, F. A.; Hawthorne, M. F.; *Inorg. Chem.* **1996**, *35*, 5417. [Crossref]
95. Kaszynski, P.; Pakhomov, S.; Tesh, K. F.; Young, V. G.; *Inorg. Chem.* **2001**, *40*, 6622. [Crossref]
96. Drechsel, K.; Lee, C. S.; Leung, E. W.; Kane, R. R.; Hawthorne, M. F.; *Tetrahedron Lett.* **1994**, *35*, 6217. [Crossref]
97. Woodhouse, S. L.; Rendina, L. M.; *Chem. Commun.* **2001**, 2464. [Crossref]
98. Naeslund, C.; Ghirmai, S.; Sjöberg, S.; *Tetrahedron* **2005**, *61*, 1181. [Crossref]
99. Ujváry, I.; Nachman, R. J.; *Peptides* **2001**, *22*, 287. [Crossref]
100. Ujváry, I.; Nachman, R. J.; *Tetrahedron Lett.* **1999**, *40*, 5147. [Crossref]
101. Zakharkin, L. I.; Kovderov, A. I.; Ol'shevskaya, V. A.; *Russ. Chem. Bull.* **1986**, *35*, 1260. [Crossref]
102. Coult, R.; Fox, M. A.; Gill, W. R.; Herbertson, P. L.; MacBride, J. A. H.; Wade, K.; *J. Organomet. Chem.* **1993**, *462*, 19. [Crossref]
103. Fujii, S.; Goto, T.; Ohta, K.; Hashimoto, Y.; Suzuki, T.; Ohta, S.; Endo, Y.; *J. Med. Chem.* **2005**, *48*, 4654. [Crossref]
104. Batsanov, A. S.; Fox, M. A.; Howard, J. A. K.; MacBride, J. A. H.; Wade, K.; *J. Organomet. Chem.* **2000**, *610*, 20. [Crossref]
105. Fox, M. A.; Cameron, A. M.; Low, P. J.; Paterson, M. A. J.; Batsanov, A. S.; Goeta, A. E.; Rankin, D. W. H.; Robertson, H. E.; Schirlin, J. T.; *Dalton Trans.* **2006**, *29*, 3544. [Crossref]
106. Dupont, J. A.; Hawthorne, M. F.; *J. Am. Chem. Soc.* **1964**, *86*, 1643. [Crossref]
107. Stadlbauer, S.; Lonnecke, P.; Welzel, P.; Hey-Hawkins, E.; *Eur. J. Org. Chem.* **2010**, *2010*, 3129. [Crossref]
108. Yang, X.; Jiang, W.; Knobler, C. B.; Hawthorne, M. F.; *J. Am. Chem. Soc.* **1992**, *114*, 9719. [Crossref]
109. Yang, X.; Jiang, W.; Knobler, C. B.; Mortimer, M. D.; Hawthorne, M. F.; *Inorg. Chim. Acta* **1995**, *240*, 371. [Crossref]
110. Zakharkin, L. I.; Kalinin, V. N.; Gedymin, V. V.; *Russ. Chem. Bull.* **1976**, *25*, 1583. [Crossref]
111. Ren, S.; Xie, Z.; *Organometallics* **2008**, *27*, 5167. [Crossref]
112. Viñas, C.; Benakki, R.; Teixidor, F.; Casabo, J.; *Inorg. Chem.* **1995**, *34*, 3844. [Crossref]
113. Kasar, R. A.; Knudsen, G. M.; Kahl, S. B.; *Inorg. Chem.* **1999**, *38*, 2936. [Crossref]

114. Venkatasubramanian, U.; Donohoe, D. J.; Ellis, D.; Giles, B. T.; Macgregor, S. A.; Robertson, S.; Rosair, G. M.; Welch, A. J.; Batsanov, A. S.; Boyd, L. A.; Copley, R. C. B.; Fox, M. A.; Howard, J. A. K.; Wade, K.; *Polyhedron* **2004**, *23*, 629. [Crossref]
115. Kiran, B.; Anoop, A.; Jemmis, E. D.; *J. Am. Chem. Soc.* **2002**, *124*, 4402. [Crossref]
116. Zhao, D.; Xie, Z.; *Coord. Chem. Rev.* **2016**, *314*, 14. [Crossref]
117. Qiu, Z.; Xie, Z.; *Chem. Soc. Rev.* **2022**, *51*, 3164. [Crossref]
118. Pelter, A.; Pardasani, R. T.; Pardasani, P.; *Tetrahedron* **2000**, *56*, 7339. [Crossref]
119. Lanfranco, A.; Renzi, P.; Rusconi, M.; Deagostino, A.; *Tetrahedron Lett.* **2023**, *131*, 154782. [Crossref]
120. Ni, H.; Qiu, Z.; Xie, Z.; *Angew. Chem., Int. Ed. Engl.* **2017**, *56*, 712. [Crossref]
121. Ni, H.; Lu, Z.; Xie, Z.; *J. Am. Chem. Soc.* **2020**, *142*, 18661. [Crossref]
122. Li, S.; Zhang, J.; Xie, Z.; *Org. Lett.* **2022**, *24*, 7497. [Crossref]
123. Liu, Q.; Zhang, B. B.; Sheng, H.; Qiao, S.; Wang, Z. X.; Chen, X. Y.; *Angew. Chem., Int. Ed. Engl.* **2023**, *62*, e202305088. [Crossref]
124. Zhang, Z. Q.; Sang, Y. Q.; Wang, C. Q.; Dai, P.; Xue, X. S.; Piper, J. L.; Peng, Z. H.; Ma, J. A.; Zhang, F. G.; Wu, J.; *J. Am. Chem. Soc.* **2022**, *144*, 14288 [Crossref]; Ren, H.; Zhang, P.; Xu, J.; Ma, W.; Tu, D.; Lu, C. S.; Yan, H.; *J. Am. Chem. Soc.* **2023**, *145*, 7838. [Crossref]
125. Scholz, M.; Hey-Hawkins, E.; *Chem. Rev.* **2011**, *111*, 7035. [Crossref]
126. Dziedzic, R. M.; Spokoyny, A. M.; *Chem. Commun.* **2019**, *55*, 430. [Crossref]
127. Kelemen, Z.; Pepiol, A.; Lupu, M.; Sillanpää, R.; Hänninen, M. M.; Teixidor, F.; Viñas, C.; *Chem. Commun.* **2019**, *55*, 8927. [Crossref]
128. Xie, Z.; Jin, G. X.; *Dalton Trans.* **2014**, *43*, 4924. [Crossref]
129. Olid, D.; Núñez, R.; Viñas, C.; Teixidor, F.; *Chem. Soc. Rev.* **2013**, *42*, 3318. [Crossref]
130. Cheng, R.; Qiu, Z.; Xie, Z.; *Nat. Commun.* **2017**, *8*, 14827. [Crossref]
131. Li, C. X.; Zhang, H. Y.; Wong, T. Y.; Cao, H. J.; Yan, H.; Lu, C. S.; *Org. Lett.* **2017**, *19*, 5178. [Crossref]
132. Xu, T. T.; Cao, K.; Zhang, C. Y.; Wu, J.; Ding, L. F.; Yang, J.; *Org. Lett.* **2019**, *21*, 9276. [Crossref]
133. Cheng, R.; Qiu, Z.; Xie, Z.; *Chem. Eur. J.* **2020**, *26*, 7212. [Crossref]
134. Cheng, R.; Qiu, Z.; Xie, Z.; *Chin. J. Chem.* **2020**, *38*, 1575. [Crossref]
135. Quan, Y.; Xie, Z.; *J. Am. Chem. Soc.* **2014**, *136*, 15513. [Crossref]
136. Lyu, H.; Quan, Y.; Xie, Z.; *Angew. Chem., Int. Ed.* **2015**, *54*, 10623. [Crossref]
137. Zhang, C.; Wang, Q.; Tian, S.; Zhang, J.; Li, J.; Zhou, L.; Lu, J.; *Org. Biomol. Chem.* **2020**, *18*, 4723. [Crossref]
138. Quan, Y.; Xie, Z.; *Angew. Chem., Int. Ed.* **2016**, *55*, 1295. [Crossref]
139. Au, Y. K.; Quan, Y.; Xie, Z.; *Chem. Asian J.* **2020**, *15*, 2170. [Crossref]
140. Chen, Y.; Au, Y. K.; Quan, Y.; Xie, Z.; *Sci. China Chem.* **2019**, *62*, 74. [Crossref]
141. Zhang, X.; Zheng, H.; Li, J.; Xu, F.; Zhao, J.; Yan, H.; *J. Am. Chem. Soc.* **2017**, *139*, 14511. [Crossref]
142. Quan, Y.; Lyu, H.; Xie, Z.; *Chem. Commun.* **2017**, *53*, 4818. [Crossref]
143. Quan, Y.; Tang, C.; Xie, Z.; *Chem. Sci.* **2016**, *7*, 5838. [Crossref]
144. Wang, Q.; Tian, S.; Zhang, C.; Li, J.; Wang, Z.; Du, Y.; Zhou, L.; Lu, J.; *Org. Lett.* **2019**, *21*, 8018. [Crossref]
145. Cao, K.; Zhang, C. Y.; Xu, T. T.; Wu, J.; Ding, L. F.; Jiang, L.; Yang, J.; *J. Organomet. Chem.* **2019**, *902*, 120956. [Crossref]
146. Au, Y. K.; Lyu, H.; Quan, Y.; Xie, Z.; *J. Am. Chem. Soc.* **2020**, *142*, 6940. [Crossref]
147. Lyu, H.; Quan, Y.; Xie, Z.; *J. Am. Chem. Soc.* **2016**, *138*, 12727. [Crossref]
148. Lyu, H.; Quan, Y.; Xie, Z.; *Chem. Eur. J.* **2017**, *23*, 14866. [Crossref]
149. Chen, Y.; Quan, Y.; Xie, Z.; *Chem. Commun.* **2020**, *56*, 12997. [Crossref]
150. Qiu, Z.; Quan, Y.; Xie, Z.; *J. Am. Chem. Soc.* **2013**, *135*, 12192. [Crossref]
151. Xu, T. T.; Zhang, C. Y.; Cao, K.; Wu, J.; Jiang, L.; Li, J.; Li, B.; Yang, J.; *ChemistrySelect* **2017**, *2*, 3396. [Crossref]
152. Wu, J.; Cao, K.; Xu, T. T.; Zhang, X. J.; Jiang, L.; Yang, J.; Huang, Y.; *RSC Adv.* **2015**, *5*, 91683. [Crossref]
153. Cao, K.; Huang, Y.; Yang, J.; Wu, J.; *Chem. Commun.* **2015**, *51*, 7257. [Crossref]
154. Cao, K.; Xu, T. T.; Wu, J.; Jiang, L.; Yang, J.; *Chem. Commun.* **2016**, *52*, 11446. [Crossref]
155. Zhao, D.; Xie, Z.; *Angew. Chem.* **2016**, *128*, 3218. [Crossref]
156. Li, S.; Xie, Z.; *J. Am. Chem. Soc.* **2022**, *144*, 7960. [Crossref]
157. Venable, T. L.; Hutton, W. C.; Grimes, R. N.; *J. Am. Chem. Soc.* **1984**, *106*, 29 [Crossref]; Reynhardt, E. C.; *J. Mag. Res.* **1986**, *69*, 337 [Crossref]; Leites, L. A.; *Chem. Rev.* **1992**, *92*, 279 [Crossref]; Sivaev, I. B.; Anufriev, S. A.; Shmalko, A. V.; *Inorg. Chim. Acta* **2023**, *547*, 121339. [Crossref]
158. Hermanek, S.; *Chem. Rev.* **1992**, *92*, 325. [Crossref]
159. Todd, L. J.; Siedle, A. R.; Bodner, G. M.; Kahl, S. B.; Hickey, J. P.; *J. Magn. Reson.* **1976**, *23*, 301. [Crossref]
160. Diaz, M.; Jaballas, J.; Arias, J.; Lee, H.; Onak, T.; *J. Am. Chem. Soc.* **1996**, *118*, 4405. [Crossref]
161. Leites, L. A.; Vinogradova, L. E.; Aleksanyan, V. I.; Bukalov, S. S.; *Russ. Chem. Bull.* **1976**, *25*, 2311. [Crossref]
162. Ditter, J. F.; Gerhart, F. J.; Williams, R. E. In *Mass Spectrometry in Inorganic Chemistry*; Margrave, J. L., ed.; American Chemical Society: US, 1968, ch. 14 [Crossref]; Vasyukova, N. I.; Nekrasov, Y. S.; Sukharev, Y. N.; Mazunov, V. A.;

Sergeev, Y. L.; *Russ. Chem. Bull.* **1985**, *34*, 1223 [Crossref]; SCIENTIFIC INSTRUMENT SERVICES (SIS), *Isotope Distribution Calculator and Mass Spec Plotter*, https://www.sisweb.com/mstools/isotope.htm, accessed in June 2024.

163. Leśnikowski, Z. J.; *Expert Opin. Drug Discovery* **2016**, *11*, 569. [Crossref]
164. Braun, S.; Jelača, S.; Laube, M.; George, S.; Hofmann, B.; Lönnecke, P.; Steinhilber, D.; Pietzsch, J.; Mijatović, S.; Maksimović-Ivanić, D.; Hey-Hawkins, E.; *Molecules* **2023**, *28*, 4547. [Crossref]
165. Zhang, J.; Pitto-Barry, A.; Shang, L.; Barry, N. P. E.; *R. Soc. Open Sci.* **2017**, *4*, 170786. [Crossref]
166. Alpatova, V. M.; Rys, E. G.; Kononova, E. G.; Khakina, E. A.; Markova, A. A.; Shibaeva, A. V.; Kuzmin, V. A.; Ol'shevskaya, V. A.; *Molecules* **2022**, *27*, 6200. [Crossref]
167. Stockmann, P.; Kuhnert, L.; Zörner, L.; Honscha, W.; Hey-Hawkins, E.; *ChemMedChem* **2023**, *18*, e202300094 [Crossref]; Stockmann, P.; Kuhnert, L.; Krajnović, T.; Mijatović, S.; Maksimović-Ivanić, D.; Honscha, W.; Hey-Hawkins, E.; *ChemMedChem.* **2023**, e202300506. [Crossref]
168. Kuhnert, K.; Kuhnert, L.; Sárosi, M. B.; George, S.; Draca, D.; Paskas, S.; Hofmann, B.; Steinhilber, D.; Honscha, W.; Mijatović, S.; Maksimović-Ivanić, D.; Hey-Hawkins, E.; *ChemMedChem* **2022**, *17*, e202100588 [Crossref]; Kuhnert, L.; Kuhnert, R.; Sárosi, M. B.; Lakoma, C.; Scholz, B. K.; Lönnecke, P.; Hey-Hawkins, E.; Honscha, W.; *Mol. Oncol.* **2023**, *18*, 280. [Crossref]
169. For selected examples, see: Tamat, S. R.; Moore, D. E.; Patwardhan, A.; Hersey, P.; *Pigm. Cell Res.* **1989**, *2*, 278 [Crossref]; Varadarajan, A.; Sharkey, R. M.; Goldenberg, D. M.; Hawthorne, M. F.; *Bioconjugate Chem.* **1991**, *2*, 102 [Crossref]; Paxton, R. J.; Beatty, B. G.; Varadarajan, A.; Hawthorne, M. F.; *Bioconjugate Chem.* **1992**, *3*, 241 [Crossref]; Chen, C. J.; Kane, R. R.; Primus, F. J.; Szalai, G.; Hawthorne, M. F.; Shively, J. E.; *Bioconjug. Chem.* **1994**, *5*, 557. [Crossref]
170. Leukart, O.; Caviezel, M.; Eberle, A.; Escher, E.; Tun-Kyi, A.; Schwyzer, R.; *Helv. Chim. Acta* **1976**, *59*, 2184 [Crossref]; Fauchkre, J. L.; Leukart, O.; Eberle, A.; Schwyzer, R.; *Helv. Chim. Acta* **1979**, *62*, 1385 [Crossref]; Pettersson, O. A.; Olsson, P.; Lindström, P.; Sjöberg, S.; Larsson, B. S.; Carlsson, J.; *Acta Oncol.* **1994**, *33*, 685 [Crossref]; Yong, J. H.; Barth, R. F.; Wyzlic, I. M.; Soloway, A. H.; Rotaru, J. H.; *Anticancer Res.* **1995**, *15*, 2033. [PubMed]
171. For selected examples, see: Wilbur, D. S.; Hamlin, D. K.; Livesey, J. C.; Srivastava, R. R.; Laramore, G. E.; Griffin, T. W.; *Nucl. Med. Biol.* **1994**, *21*, 601 [Crossref]; Morris, J. H.; Peters, G. S.; Koldaeva, E.; Spryshkova, R.; Borisov, G.; *Appl. Organomet. Chem.* **1995**, *9*, 323 [Crossref]; Wood, P. J.; Scobie, M.; Threadgill, M. D.; *Int. J. Radiat. Biol.* **1996**, *70*, 587. [Crossref]
172. For selected examples, see: Jarugula, V. R.; Schinazi, R. F.; Fulcrand, G.; El Kattan, Y.; Liotaii, D. C.; Boudinot, F. D.; *J. Pharm. Sci.* **1994**, *86*, 1697 [Crossref]; Goudgaon, N. M.; El-Kattan, Y. A.; Xia, X.; McAtee, J.; Soria, J.; Wey, S. J.; Liotta, D. C.; Schinazi, R. F.; *Nucleosides Nucleotides* **1997**, *16*, 2133 [Crossref]; Mourier, N. S.; Eleuteri, A.; Hurwitz, S. J.; Tharnish, P. M.; Schinazi, R. F.; *Bioorg. Med. Chem.* **1999**, *7*, 2759 [Crossref]; Schinazi, R. F.; Hurwitz, S. J.; Liberman, I.; Juodawlkis, A. S.; Tharnish, P.; Shi, J.; Liotta, D. C.; A Coderre, J.; Olson, J.; *Clin. Cancer Res.* **2000**, *6*, 725 [Crossref]; Yan, J.; Naeslund, C.; Al-Madhoun, A. S.; Wang, J.; Ji, W.; Cosquer, G. Y.; Johnsamuel, J.; Sjöberg, S.; Eriksson, S.; Tjarks, W.; *Bioorg. Med. Chem. Lett.* **2002**, *12*, 2209 [Crossref]; Olejniczak, A. B.; Koziolkiewicz, M.; Lesnikowski, Z. J.; *Antisense Nucleic Acid Drug Dev.* **2002**, *12*, 79 [Crossref]; Johnsamuel, J.; Lakhi, N.; Al-Madhoun, A. S.; Byun, Y.; Yan, J.; Eriksson, S.; Tjarks, W.; *Bioorg. Med. Chem.* **2004**, *12*, 4769 [Crossref]; Schinazi, R. F.; Hurwitz, S. J.; Liberman, I.; Glazkova, Y.; Mourier, N. S.; Olson, J.; Keane, T.; *Nucleosides Nucleotides Nucleic Acids* **2004**, *23*, 291 [Crossref]; Barth, R. F.; Yang, W.; Al-Madhoun, A. S.; Johnsamuel, J.; Byun, Y.; Chandra, S.; Smith, D. R.; Tjarks, W.; Eriksson, S.; *Cancer Res.* **2004**, *64*, 6287 [Crossref]; Binello, E.; Mitchell, R. N.; Harling, O. K.; *Appl. Radiat. Isot.* **2004**, *61*, 959 [Crossref]; Leśnikowski, Z. J.; Paradowska, E.; Olejniczak, A. B.; Studzińska, M.; Seekamp, P.; Schüssler, U.; Gabel, D.; Schinazi, R. F.; Plesek, J.; *Bioorg. Med. Chem.* **2005**, *13*, 4168 [Crossref]; Byun, Y.; Thirumamagal, B. T. S.; Yang, W.; Eriksson, S.; Barth, R. F.; Tjarks, W.; *J. Med. Chem.* **2006**, *49*, 5513 [Crossref]; Reynolds, R. C.; Campbell, S. R.; Fairchild, R. G.; Kisliuk, R. L.; Micca, P. L.; Queener, S. F.; Riordan, J. M.; Sedwick, W. D.; Waud, W. R.; Leung, A. K. W.; Dixon, R. W.; Suling, W. J.; Borhani, D. W.; *J. Med. Chem.* **2007**, *50*, 3283 [Crossref]; Barth, R. F.; Yang, W.; Wu, G.; Swindall, M.; Byun, Y.; Narayanasamy, S.; Tjarks, W.; Tordoff, K.; Moeschberger, M. L.; Eriksson, S.; Binns, P. J.; Riley, K. J.; *Proc. Natl. Acad. Sci. U. S. A.* **2008**, *105*, 17493 [Crossref]; Druzina, A. A.; Bregadze, V. I.; Mironov, A. F.; Semioshkin, A. A.; *Russ. Chem. Rev.* **2016**, *85*, 1229. [Crossref]
173. For selected examples, see: Ahrens, V. M.; Frank, R.; Stadlbauer, S.; Beck-Sickinger, A. G.; Hey-Hawkins, E.; *J. Med. Chem.* **2011**, *54*, 2368 [Crossref]; Kimura, S.; Masunaga, S. I.; Harada, T.; Kawamura, Y.; Ueda, S.; Okuda, K.; Nagasawa, H.; *Bioorg. Med. Chem.* **2011**, *19*, 1721 [Crossref]; El-Zaria, M. E.; Genady, A. R.; Janzen, N.; Petlura, C. I.; Beckford Vera, D. R.; Valliant, J. F.; *Dalton Trans.* **2014**, *43*, 4950 [Crossref]; Frank, R.; Ahrens, V. M.; Boehnke, S.; Beck-Sickinger, A. G.; Hey-Hawkins, E.; *ChemBioChem* **2016**, *17*, 308 [Crossref]; Worm, D. J.; Els-Heindl, S.; Kellert, M.; Kuhnert, R.; Saretz, S.; Koebberling, J.; Riedl, B.; Hey-Hawkins, E.; Beck-Sickinger, A. G.; *J. Pept. Sci.* **2018**, *24*, e3119 [Crossref]; Wang, S.; Blaha, C.; Santos, R.; Huynh, T.; Hayes, T. R.; Beckford-Vera, D. R.; Blecha, J. E.; Hong, A. S.; Fogarty, M.; Hope, T. A.; Raleigh, D. R.; Wilson, D. M.; Evans, M. J.; VanBrocklin, H. F.; Ozawa,

T.; Flavell, R. R.; *Mol. Pharm.* **2019**, *16*, 3831 [Crossref]; He, T.; Chittur, S. V.; Musah, R. A.; *ACS Chem. Neurosci.* **2019**, *10*, 1524 [Crossref]; Worm, D. J.; Hoppenz, P.; Els-Heindl, S.; Kellert, M.; Kuhnert, R.; Saretz, S.; Köbberling, J.; Riedl, B.; Hey-Hawkins, E.; Beck-Sickinger, A. G.; *J. Med. Chem.* **2020**, *63*, 2358 [Crossref]; Hoppenz, P.; Els-Heindl, S.; Kellert, M.; Kuhnert, R.; Saretz, S.; Lerchen, H. G.; Köbberling, J.; Riedl, B.; Hey-Hawkins, E.; Beck-Sickinger, A. G.; *J. Org. Chem.* **2020**, *85*, 1446. [Crossref]

174. For selected examples, see: Jacobsson, M.; Winander, C.; Mani, K.; Ellervik, U.; *Bioorg. Med. Chem. Lett.* **2008**, *18*, 2451 [Crossref]; Lai, C. H.; Lin, Y. C.; Chou, F. I.; Liang, C. F.; Lin, E. W.; Chuang, Y. J.; Lin, C. C.; *Chem. Commun.* **2012**, *48*, 612 [Crossref]; Satapathy, R.; Dash, B. P.; Bode, B. P.; Byczynski, E. A.; Hosmane, S. N.; Bux, S.; Hosmane, N. S.; *Dalton Trans.* **2012**, *41*, 8982 [Crossref]; Zhang, T.; Li, G.; Li, S.; Wang, Z.; He, D.; Wang, Y.; Zhang, J.; Li, J.; Bai, Z.; Zhang, Q.; Liu, B.; Zhao, Q.; Liu, Y.; Zhang, H.; *Colloids Surf., B* **2019**, *182*, 110397. [Crossref]
175. For selected examples, see: Cappelli, A.; Valenti, S.; Mancini, A.; Giuliani, G.; Anzini, M.; Altieri, S.; Bortolussi, S.; Ferrari, C.; Clerici, A. M.; Zonta, C.; Carraro, F.; Filippi, I.; Giorgi, G.; Donati, A.; Ristori, S.; Vomero, S.; Concas, A.; Biggio, G.; *Bioconjug. Chem.* **2010**, *21*, 2213 [Crossref]; Crossley, E. L.; Issa, F.; Scarf, A. M.; Kassiou, M.; Rendina, L. M.; *Chem. Commun.* **2011**, *47*, 12179 [Crossref]; Narlawar, R.; Austin, C. J. D.; Kahlert, J.; Selleri, S.; Da Pozzo, E.; Martini, C.; Werry, E. L.; Rendina, L. M.; Kassiou, M.; *Chem. Asian J.* **2018**, *13*, 3321. [Crossref]
176. For selected examples, see: Ioppolo, J. A.; Kassiou, M.; Rendina, L. M.; *Tetrahedron Lett.* **2009**, *50*, 6457 [Crossref]; Genady, A. R.; *Eur. J. Med. Chem.* **2009**, *44*, 409 [Crossref]; Alberti, D.; Toppino, A.; Geninatti Crich, S.; Meraldi, C.; Prandi, C.; Protti, N.; Bortolussi, S.; Altieri, S.; Aime, S.; Deagostino, A.; *Org. Biomol. Chem.* **2014**, *12*, 2457 [Crossref]; Otero, R.; Seoane, S.; Sigüeiro, R.; Belorusova, A. Y.; Maestro, M. A.; Pérez-Fernández, R.; Rochel, N.; Mouriño, A.; *Chem. Sci.* **2016**, *7*, 1033 [Crossref]; Alberti, D.; Michelotti, A.; Lanfranco, A.; Protti, N.; Altieri, S.; Deagostino, A.; Geninatti Crich, S.; *Sci. Rep.* **2020**, *10*, 19274 [Crossref]; Druzina, A. A.; Zhidkova, O. B.; Dudarova, N. V.; Nekrasova, N. A.; Suponitsky, K. Y.; Timofeev, S. V.; Bregadze, V. I.; *Molecules* **2021**, *26*, 6687 [Crossref]; Chen, J.; Dai, Q.; Yang, Q. Y.; Bao, X.; Zhou, Y.; Zhong, H.; Wu, L.; Wang, T.; Zhang, Z.; Lu, Y.; Zhang, Z.; Lin, M.; Han, M.; Wei, Q.; *J. Nanobiotechnol.* **2022**, *20*, 102. [Crossref]
177. Dumelin, C. E.; Trüssel, S.; Buller, F.; Trachsel, E.; Bootz, F.; Zhang, Y.; Mannocci, L.; Beck, S. C.; Drumea-Mirancea, M.; Seeliger, M. W.; Baltes, C.; Müggler, T.; Kranz, F.; Rudin, M.; Melkko, S.; Scheuermann, J.; Neri, D.; *Angew. Chem., Int. Ed.* **2008**, *47*, 3196. [Crossref]
178. Nishimura, K.; Harrison, S.; Kawai, K.; Morita, T.; Miura, K.; Okada, S.; Nakamura, H.; *Bioorg. Med. Chem. Lett.* **2022**, *72*, 128869. [Crossref]
179. Fujikawa, Y.; Fukuo, Y.; Nishimura, K.; Tsujino, K.; Kashiwagi, H.; Hiramatsu, R.; Nonoguchi, N.; Furuse, M.; Takami, T.; Hu, N.; Miyatake, S. I.; Takata, T.; Tanaka, H.; Watanabe, T.; Suzuki, M.; Kawabata, S.; Nakamura, H.; Wanibuchi, M.; *Biology* **2023**, *12*, 1240 [Crossref]; Nishimura, K.; Kashiwagi, H.; Morita, T.; Fukuo, y.; Okada, S.; Miura, K.; Matsumoto, Y.; Sugawara, Y.; Enomoto, T.; Suzuki, M.; Nakai, K.; Kawabata, S.; Nakamura, H.; *J. Controlled Release* **2023**, *360*, 249. [Crossref]
180. Matović, J.; Järvinen, J.; Bland, H. C.; Sokka, I. K.; Imlimthan, S.; Ferrando, R. M.; Huttunen, K. M.; Timonen, J.; Peräniemi, S.; Aitio, O.; Airaksinen, A. J.; Sarparanta, M.; Johansson, M. P.; Rautio, J.; Ekholm, F. S.; *Mol. Pharmaceutics* **2020**, *17*, 3885 [Crossref]; Matović, J.; Järvinen, J.; Sokka, I. K.; Imlimthan, S.; Raitanen, J. E.; Montaser, A.; Maaheimo, H.; Huttunen, K. M.; Peräniemi, S.; Airaksinen, A. J.; Sarparanta, M.; Johansson, M. P.; Rautio, J.; Ekholm, F. S.; *Mol. Pharm.* **2021**, *18*, 285 [Crossref]; Matović, J.; Järvinen, J.; Sokka, I. K.; Stockmann, P.; Kellert, M.; Imlimthan, S.; Sarparanta, M.; Johansson, M. P.; Hey-Hawkins, E.; Rautio, J.; Ekholm, F. S.; *ACS Omega* **2022**, *7*, 30376. [Crossref]
181. Couto, M.; Mastandrea, I.; Cabrera, M.; Cabral, P.; Teixidor, F.; Cerecetto, H.; Viñas, C.; *Chemistry* **2017**, *23*, 9233. [Crossref]
182. Couto, M.; Alamón, C.; García, M. F.; Kovacs, M.; Trias, E.; Nievas, S.; Pozzi, E.; Curotto, P.; Thorp, S.; Dagrosa, M. A.; Teixidor, F.; Viñas, C.; Cerecetto, H.; *Cells* **2020**, *9*, 1408. [Crossref]
183. Couto, M.; Alamón, C.; Nievas, S.; Perona, M.; Dagrosa, M. A.; Teixidor, F.; Cabral, P.; Viñas, C.; Cerecetto, H.; *Chemistry* **2020**, *26*, 14335. [Crossref]
184. Couto, M.; García, M. F.; Alamón, C.; Cabrera, M.; Cabral, P.; Merlino, A.; Teixidor, F.; Cerecetto, H.; Viñas, C.; *Chemistry* **2018**, *24*, 3122. [Crossref]
185. Alamón, C.; Dávila, B.; García, M. F.; Sánchez, C.; Kovacs, M.; Trias, E.; Barbeito, L.; Gabay, M.; Zeineh, N.; Gavish, M.; Teixidor, F.; Viñas, C.; Couto, M.; Cerecetto, H.; *Cancers* **2020**, *12*, 3423. [Crossref]
186. Alamón, C.; Dávila, B.; García, M. F.; Nievas, S.; Dagrosa, M. A.; Thorp, S.; Kovacs, M.; Trias, E.; Faccio, R.; Gabay, M.; Zeineh, N.; Weizman, A.; Teixidor, F.; Viñas, C.; Gavish, M.; Cerecetto, H.; Couto, M.; *Mol Pharm.* **2023**, *20*, 2702. [Crossref]
187. Couto, M.; Alamón, C.; Sánchez, C.; Dávila, B.; Fernández, M.; Lecot, N.; Cabral, P.; Teixidor, F.; Viñas, C.; Cerecetto, H.; *Future Med. Chem.* **2019**, *11*, 2273. [Crossref]
188. Alamón, C.; Dávila, B.; Cerecetto, H.; Couto, M.; *Chem. Biol. Drug Des.* **2023**, *101*, 1435. [Crossref]
189. Ma, W.; Wang, Y.; Xue, Y.; Wang, M.; Lu, C.; Guo, W.; Liu, Y. H.; Shu, D.; Shao, G.; Xu, Q.; Tu, D.; Yan, H.; *Chem. Sci.* **2024**, *15*, 4019. [Crossref]

190. Li, R.; Zhang, J.; Guo, J.; Xu, Y.; Duan, K.; Zheng, J.; Wan, H.; Yuan, Z.; Chen, H.; *Mol. Pharmaceutics* **2020**, *17*, 202. [Crossref]
191. Zhang, T.; Du, S.; Wang, Y.; Guo, Y.; Yi, Y.; Liu, B.; Liu, Y.; Chen, X.; Zhao, Q.; He, D.; Wang, Z.; Zhang, H.; Ma, Q.; *ChemistrySelect* **2020**, *5*, 14652. [Crossref]
192. Gruzdev, D. A.; Telegina, A. A.; Levit, G. L.; Solovieva, O. I.; Gusel'nikova, T. Y.; Razumov, I. A.; Krasnov, V. P.; Charushin, V. N.; *Int. J. Mol. Sci.* **2022**, *23*, 13726. [Crossref]
193. Lutz, M. R.; Flieger, S.; Colorina, A.; Wozny, J.; Hosmane, N. S.; Becker, D. P.; *ChemMedChem* **2020**, *15*, 1897 [Crossref]; Flieger, S.; Takagaki, M.; Kondo, N.; Lutz Jr., M. R.; Gupta, Y.; Ueda, H.; Sakurai, Y.; Moran, G.; Kempaiah, P.; Hosmane, N.; Suzuki, M.; Becker, D. P.; *Int. J. Mol. Sci.* **2023**, *24*, 6973. [Crossref]
194. da Silva, A. F. F.; Seixas, R. S. G. R.; Silva, A. M. S.; Coimbra, J.; Fernandes, A. C.; Santos, J. P.; Matos, A.; Rino, J.; Santos, I.; Marques, F.; *Org. Biomol. Chem.* **2014**, *12*, 5201 [Crossref]; Belchior, A.; Fernandes, A.; Lamotte, M.; da Silva, A. F. F.; Seixas, R. S. G. R.; Silva, A. M. S.; Marques, F.; *Int. J. Mol. Sci.* **2022**, *23*, 14929 [Crossref]; Druzina, A. A.; Dudarova, N. V.; Ananyev, I. V.; Antonets, A. A.; Kaluzhny, D. N.; Nazarov, A. A.; Sivaev, I. B.; Bregadze, V. I.; *Molecules* **2023**, *28*, 6636. [Crossref]
195. Kaniowski, D.; Kulik, K.; Ebenryter-Olbińska, K.; Wielgus, E.; Lesnikowski, Z.; Nawrot, B.; *Biomolecules* **2020**, *10*, 718 [Crossref]; Kaniowski, D.; Suwara, J.; Ebenryter-Olbińska, K.; Jakóbik-Kolon, A.; Nawrot, B.; *Int. J. Mol. Sci.* **2022**, *23*, 14793 [Crossref]; Shirakawa, M.; Zaboronok, A.; Nakai, K.; Sato, Y.; Kayaki, S.; Sakai, T.; Tsurubuchi, T.; Yoshida, F.; Nishiyama, T.; Suzuki, M.; Tomida, H.; Matsumura, A.; *Cells* **2021**, *10*, 3421 [Crossref]; Kawasaki, R.; Hirano, H.; Yamana, K.; Isozaki, H.; Kawamura, S.; Sanada, Y.; Bando, K.; Tabata, A.; Yoshikawa, K.; Azuma, H.; Takata, T.; Tanaka, H.; Sakurai, Y.; Suzuki, M.; Tarutani, N.; Katagiri, K.; Sawada, S. I.; Sasaki, Y.; Akiyoshi, K.; Nagasaki, T.; Ikeda, A.; *Nanomedicine : Nanotechnol. Biol. Med.* **2023**, *49*, 102659. [Crossref]
196. Tarrés, M.; Canetta, E.; Paul, E.; Forbes, J.; Azzouni, K.; Viñas, C.; Teixidor, F.; Harwood, A. J.; *Sci. Rep.* **2015**, *5*, 7804 [Crossref]; He, T.; Misuraca, J. C.; Musah, R. A.; *Sci. Rep.* **2017**, *7*, 16995. [Crossref]
197. Fauchère, J. L.; Do, K. Q.; Jow, P. Y.; Hansch, C.; *Experientia* **1980**, *36*, 1203. [Crossref]
198. Rak, J.; Dejlová, B.; Lampová, H.; Kaplánek, R.; Matějíček, P.; Cígler, P.; Král, V.; *Mol. Pharm.* **2013**, *10*, 1751. [Crossref]
199. Dąbrowska, A.; Matuszewski, M.; Zwoliński, K.; Ignaczak, A.; Olejniczak, A. B.; *Eur. J. Pharm. Sci.* **2018**, *111*, 226. [Crossref]
200. Yamamoto, K.; Endo, Y.; *Bioorg. Med. Chem. Lett.* **2001**, *11*, 2389. [Crossref]
201. Endo, Y.; Yamamoto, K.; Kagechika, H.; *Bioorg. Med. Chem. Lett.* **2003**, *13*, 4089. [Crossref]
202. Goszczyński, T. M.; Fink, K.; Kowalski, K.; Leśnikowski, Z. J.; Boratyński, J.; *Sci. Rep.* **2017**, *7*, 9800. [Crossref]

Submitted: January 20, 2024
Published online: June 25, 2024